iScience

CellPress
OPEN ACCESS

Article

Prelimbic area to lateral hypothalamus circuit drives social aggression

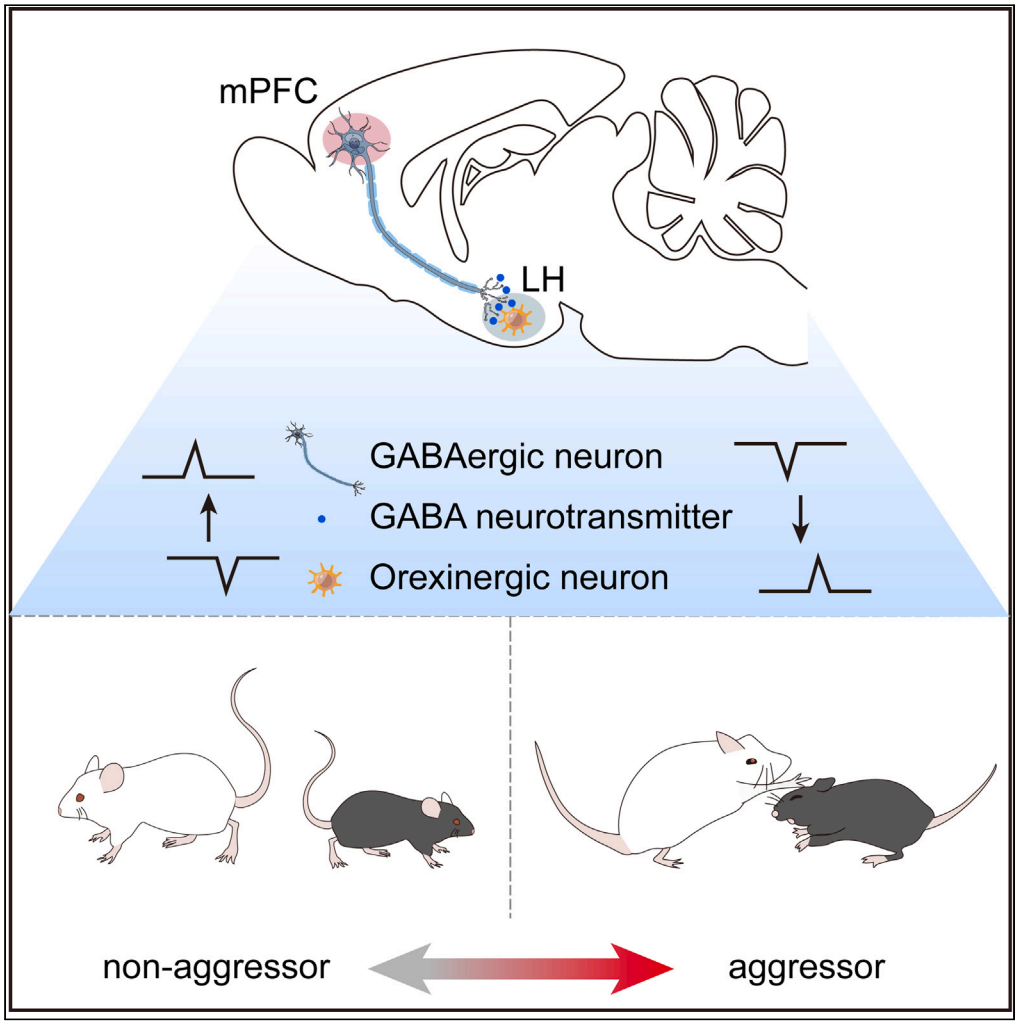

Fuhai Bai, Lu Huang, Jiao Deng, ..., Min Zhang, Ying Xiong, Hong Li

xiongying2001@163.com (Y.X.)
lh78553@163.com (H.L.)

Highlights

A portion of GABAergic neurons in the mPFC are deactivated during aggression

Activating mPFC GABAergic neurons inhibits aggression

Silencing mPFC GABAergic neurons promotes aggression

$MPFC^{GABAergic}$-$LH^{orexinergic}$ circuit participates in the regulation of aggressive behavior

Bai et al., iScience 26, 107718
October 20, 2023
https://doi.org/10.1016/j.isci.2023.107718

iScience

CellPress
OPEN ACCESS

Article

Prelimbic area to lateral hypothalamus circuit drives social aggression

Fuhai Bai,[1,8] Lu Huang,[1,8] Jiao Deng,[2] Zonghong Long,[1] Xianglin Hao,[3] Penghui Chen,[4] Guangyan Wu,[5] Huizhong Wen,[4] Qiangting Deng,[6] Xiaohang Bao,[1] Jing Huang,[1] Ming Yang,[1] Defeng Li,[7] Yukun Ren,[1] Min Zhang,[1] Ying Xiong,[4,*] and Hong Li[1,9,*]

SUMMARY

Controlling aggression is a vital skill in social species such as rodents and humans and has been associated with the medial prefrontal cortex (mPFC). In this study, we showed that during aggressive behavior, the activity of GABAergic neurons in the prelimbic area (PL) of the mPFC was significantly suppressed. Specific activation of GABAergic PL neurons significantly curbed male-to-male aggression and inhibited conditioned place preference (CPP) for aggression-paired contexts, whereas specific inhibition of GABAergic PL neurons brought about the opposite effect. Moreover, GABAergic projections from PL neurons to the lateral hypothalamus (LH) orexinergic neurons mediated aggressive behavior. Finally, directly modulated LH-orexinergic neurons influence aggressive behavior. These results suggest that GABAergic PL-orexinergic LH projection is an important control circuit for intermale aggressive behavior, both of which could be targets for curbing aggression.

INTRODUCTION

Aggression is a conserved innate behavior during evolution. However, uncontrollable aggression causes enormous problems to human society. It can also be a symptom of various neurological and psychiatric disorders, including Alzheimer's disease and a change in hormone levels.[1,2] Currently, treatment for this uncontrollable behavior is limited to non-specific psychotic medications. In order to develop a specific mitigative strategy, it is pivotal to understand the underlying neural circuit for this behavior.

The mPFC is an area known to play a pivotal role in a social hierarchy,[3–6] which is achieved by a series of territorial behaviors, including aggression and violence.[7,8] It projects to the dorsal raphe, ventral tegmental area, hypothalamus, and so forth and exerts top-down modulations on various types of neurotransmission. In human, lesion to the prefrontal cortex, especially the mPFC, have been shown to cause impulsivity and antisocial behaviors.[9–11] Brain-lesion and brain imaging studies suggest that neural circuitries of reactive aggression in humans are similar to aggression-related neural networks in rodents.[7] Nonspecific activation of the mPFC was also found to inhibit aggression behavior between males.[8] Specifically, optogenetic activation of excitatory neurons in the mPFC inhibits intermale aggression in mice. In contrast, optogenetic silencing of mPFC excitatory neurons causes an escalation of aggressive behavior both quantitatively and qualitatively.[8,12] Although these results highlight the importance of mPFC excitatory neurons in aggression, the inhibitory neurons in mPFC as well as the projections targets of mPFC neurons mediate the aggression modulatory effect remain largely unknown.

It is known that the mPFC consists of most glutamatergic excitatory projection neurons. However, there is a small population of GABAergic inhibitory neurons (10–20% in rodents).[13,14] GABAergic interneurons control information flow by targeting specific domains of principal neurons. It is believed that GABAergic interneurons regulate the timing of pyramidal cell firing, synchronize network activity, generate cortical rhythms, and regulate sensory receptive fields and plasticity. They also involve in maintaining the balance between excitatory and inhibitory impulses while preventing runaway excitations that are essential for survival.[13,15–19] Despite these studies, very little is known about the GABAergic neurons in the mPFC that are associated with aggression, including whether they provide long-range projections and where these projections lead.

In this study, we sought to characterize the cell-type-specific dynamics of PL (one of the mPFC regions) GABAergic neurons during aggression and to determine the downstream effect and neuronal specificity for the PL GABAergic modulation of aggressive behavior. First, the

[1]Department of Anesthesiology, Xinqiao Hospital, Army Medical University, Chongqing 400037, China
[2]Department of Anesthesiology and Perioperative Medicine, Xijing Hospital, Air Force Medical University, Xi'an, Shaanxi 710032, China
[3]Department of Pathology, Xinqiao Hospital, Army Medical University, Chongqing 400037, P.R. China
[4]Department of Neurobiology, Chongqing Key Laboratory of Neurobiology, Army Medical University, Chongqing 400038, China
[5]Experimental Center of Basic Medicine, College of Basic Medical Sciences, Army Medical University, Chongqing 400038, China
[6]Editorial Office of Journal of Army Medical University, Chongqing 400038, China
[7]Clinical Medical Research Center, Xinqiao Hospital, Army Medical University, Chongqing 400037, China
[8]These authors contributed equally
[9]Lead contact
*Correspondence: xiongying2001@163.com (Y.X.), lh78553@163.com (H.L.)
https://doi.org/10.1016/j.isci.2023.107718

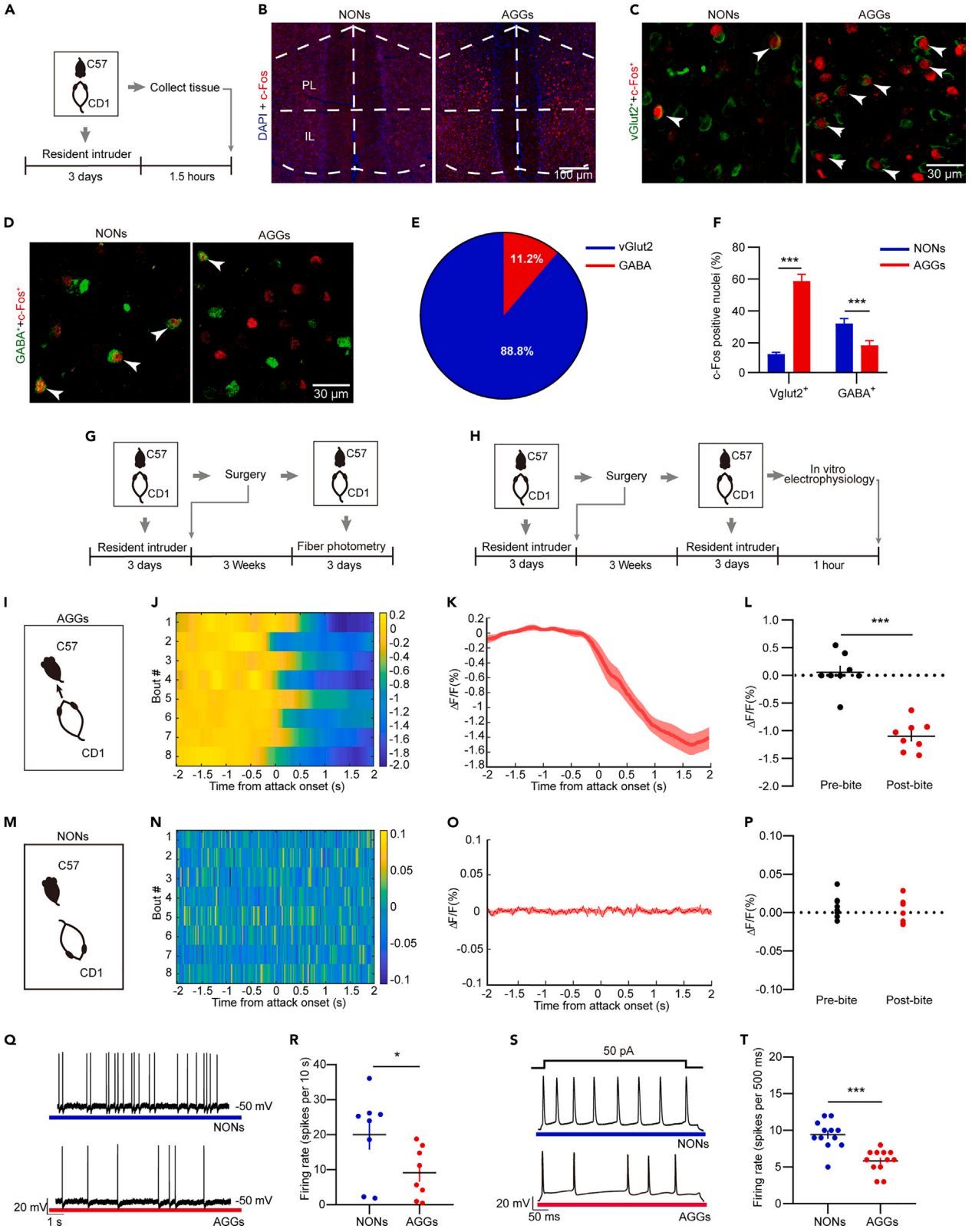
A
C57
CD1
Collect tissue
Resident intruder
3 days
1.5 hours
B
NONs
AGGs
DAPI + c-Fos
PL
IL
100 μm
C
NONs
AGGs
vGlut2+c-Fos+
30 μm
D
NONs
AGGs
GABA+c-Fos+
30 μm
E
11.2%
88.8%
vGlut2
GABA
F
c-Fos positive nuclei (%)
NONs
AGGs
***
***
Vglut2+
GABA+
G
C57
CD1
Surgery
Resident intruder
3 days
3 Weeks
Fiber photometry
3 days
H
C57
CD1
Surgery
In vitro electrophysiology
Resident intruder
3 days
3 Weeks
Resident intruder
3 days
1 hour
I
AGGs
C57
CD1
J
Bout #
Time from attack onset (s)
K
ΔF/F(%)
Time from attack onset (s)
L
ΔF/F(%)
***
Pre-bite
Post-bite
M
NONs
C57
CD1
N
Bout #
Time from attack onset (s)
O
ΔF/F(%)
Time from attack onset (s)
P
ΔF/F(%)
Pre-bite
Post-bite
Q
-50 mV
NONs
20 mV
1 s
-50 mV
AGGs
R
Firing rate (spikes per 10 s)
*
NONs
AGGs
S
50 pA
NONs
20 mV
50 ms
AGGs
T
Firing rate (spikes per 500 ms)
***
NONs
AGGs

Figure 1. Aggressive behaviors are associated with decreased PL GABAergic neuron activity

(A) Flow diagram of immunofluorescence.

(B) Representative images of immunofluorescence in the PL for c-Fos (red) and DAPI (blue) overlay in NONs and AGGs mice after RI screening (scale bar, 100 μm).

(C and D) Representative images of immunofluorescence in the PL for VGlut2 (green) (C), GABA (green) (D) and c-Fos (red) overlay in NONs and AGGs mice after RI screening (scale bar, 30 μm).

(E) Pie chart depicting percentage of PL neurons that are positive for VGlut2 or GABA as determined by immunofluorescence, n = 4 mice for each group.

(F) c-Fos$^+$ nuclei were higher in AGGs than in NONs for total and VGlut2$^+$ PL neurons and lower in GABA$^+$ LHb neurons. Two-tailed unpaired t-test, total: $p = 0.0014$; VGlut2: $p < 0.0001$; GABA: $p = 0.0202$. n = 4 mice for each group, two slices per mouse.

(G) Flow diagram of fiber photometry recording.

(H) Flow diagram of *in vitro* electrophysiology.

(I) Aggression RI schematic.

(J) Heatmap representation of $Ca2^+$ transients of GABAergic neurons in the PL evoked by aggressive behavior. Each row represents a bout. n = 8 mice.

(K) Peri-event plot of AGGs PL GABAergic neurons activity 2 s before and after a bite from an aggressive bout. The red line denotes the mean signals for all animals, whereas the pink shaded region denotes the SEM, n = 8 biologically independent mice.

(L) AGGs displayed a decrease in average GABAergic neuron activity after a bite. Two-tailed paired t-test, n = 8 biologically independent mice, 3–5 bites per mouse, $p < 0.0001$.

(M) Non-aggression RI schematic.

(N) Heatmap representation of GCaMP6m transients in NONs. n = 8 mice.

(O) Peri-event plot of NONs PL GABAergic neurons activity. The red line denotes the mean signals for all animals, whereas the pink shaded region denotes the SEM, n = 8 biologically independent mice.

(P) NONs displayed no change in average GABAergic neuron activity duration of RI testing. Two-tailed paired t-test, $p = 0.6904$. n = 8 biologically independent mice.

(Q) Spontaneous firing of GABAergic neurons recorded in the PL of NONs and AGGs with the membrane potential held at −50 mV

(R) Scatterplot representative the firing rate of GABAergic neurons in the PL firing properties of NONs and AGGs. Two-tailed unpaired t-test, $p = 0.0464$. n = 8 cells, n = 8 mice for each group.

(S) Representative firing responses to 50 pA current injections in NONs and AGGs.

(T) Representative the firing rate of GABAergic neurons in the PL firing after 50 pA current injections of NONs and AGGs. Two-tailed unpaired t-test, $p < 0.0001$. n = 12 cells, n = 8 mice for each group. *$p < 0.05$, **$p < 0.01$, ***$p < 0.001$; All data were presented as means ± SEM.

number of activated glutamatergic neurons is increased in the PL, but the number of activated GABAergic neurons is decreased during aggression, along with diminished calcium signaling in GABAergic neurons. Next, we found that direct optogenetic or chemogenetic manipulation of GABAergic PL neurons altered aggressive behavior and aggression CPP. Furthermore, we found that LH orexinergic neurons receive GABAergic projections from the PL by anterograde tracing, and GABAergic PL-LH projections could be an important target for modulating aggressive behavior. Our findings indicate that GABAergic neurons in the PL, and their projection to LH orexinergic neurons, are important components for mitigating strategies against aggression.

RESULTS

Individual differences in aggression-related behavior

To study individual differences in aggression, we used the resident intruder (RI) test model of social defeat for CD-1 mice (Figure S1A). After three consecutive days of the RI test screen, approximately 80% (32/40) of mice exhibited aggressive behavior (termed aggressors (AGGs)) during the test, and approximately 20% (8/40) failed to initiate aggressive behavior (termed non-aggressors (NONs)) during the test (Figure S1B). Ethological analysis revealed that aggression in AGGs toward the intruder was significantly increased (Figure S1C), so were the mean number of attack bouts (Figure S1D) and mean duration of attack bouts (Figure S1E), as compared to that of NONs. At the same time, the mean number of pursuit bouts (Figure S1F) and mean duration of pursuit bouts (Figure S1G) were also significantly increased in AGGs vs. NONs.

Recent animal studies have shown that highly aggressive male mice use levers to force access to subordinate intruders[20] and form a CPP for contexts associated with access to subordinate intruders.[2,21] To assay the aggressive state of CD-1 mice, we also used a CPP model by receiving novel C57BL/6J intruder-paired or intruder-unpaired sessions twice a day for three continuous days after aggression screening (Figures S1A and S1H). AGGs exhibited a CPP for the intruder-paired context, while NONs displayed conditioned place aversion (CPA, Figures S1I–S1K). In addition, we tested the time spent in the center of an open field to determine the anxiety level (Figures S1L and S1M). These results indicated that the CPP or CPA effects were not mediated by changes in overall activity or anxiety. After behavioral testing, the corticosterone level was decreased (Figure S1N), and the testosterone level was elevated (Figure S1O) in AGGs, suggesting that AGGs may be more dominant than NONs stressed by forced intruder interactions.

Aggression is associated with decreased prelimbic GABAergic neuron activity

To look for aggressively activated nuclei, we first performed the RI paradigm for 10 min and then examined the whole brain for c-Fos expression. The c-Fos expression was dramatically increased throughout the brain under aggression, and we observed a marked accumulation of strong c-Fos$^+$ neurons in the PL. Considering that PL is involved in the acute and chronic regulation of social dominance,[5,6,22] we focus here on the PL during aggression. Specifically, 1.5 h after the end of the RI test on day 3 (Figure 1A), we found the number of c-Fos$^+$ neurons in the PL of

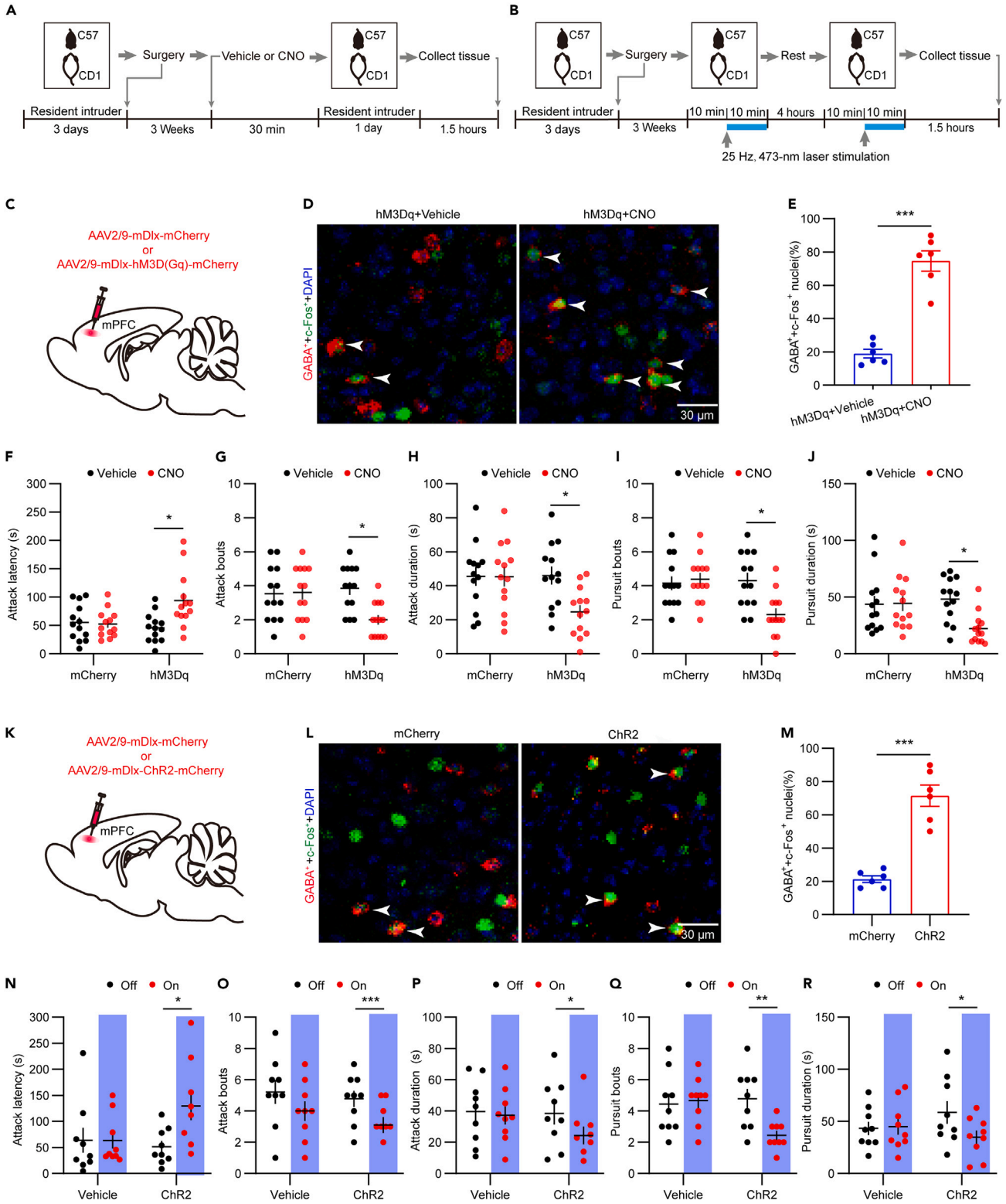

Figure 2. Opto and chemogenetics activation of PL GABAergic neurons reduced aggressive behaviors

(A) Flowchart of a chemogenetic activation experiment.

(B) Flowchart of an optogenetics activation experiment.

(C) Surgical manipulations and representative viral infection for GABAergic neuron in the PL.

Figure 2. *Continued*

(D) Representative images of immunofluorescence for c-Fos (green), mCherry (red) and DAPI (blue) in hM3Dq+Vehicle group and hM3Dq+CNO group (scale bar, 30 μm).

(E) CNO treatment increased the percent of c-Fos+ and GABA+ co-expression neurons in hM3Dq+CNO group compared to hM3Dq+Vehicle group. Two-tailed unpaired t-test, $p < 0.0001$. n = 6 mice for each group.

(F) hM3Dq-mediated stimulation of GABAergic PL neurons increased attack latency after CNO treatment in RI. two-way ANOVA, $p = 0.0211$. n = 13 mice for each group.

(G) hM3Dq-mediated stimulation of GABAergic PL neurons reduced attack bouts after CNO treatment in RI. two-way ANOVA, $p = 0.0271$. n = 13 mice for each group.

(H) hM3Dq-mediated stimulation of GABAergic PL neurons reduced attack duration after CNO treatment in RI. two-way ANOVA, $p = 0.0406$. n = 13 mice for each group.

(I) hM3Dq-mediated stimulation of GABAergic PL neurons reduced pursuit bouts after CNO treatment in RI. two-way ANOVA, $p = 0.0322$. n = 13 mice for each group.

(J) hM3Dq-mediated stimulation of GABAergic PL neurons reduced pursuit duration after CNO treatment in RI. two-way ANOVA, $p = 0.0362$. n = 13 mice for each group.

(K) Surgical manipulations and representative viral infection for GABAergic neuron in the PL.

(L) Representative images of immunofluorescence for c-Fos (green), mCherry (red) and DAPI (blue) in mCherry group and ChR2 group (scale bar, 30 μm).

(M) Blue light increased the percent of c-Fos+ and GABA+ co-expression neurons in ChR2 group compared to mCherry group. Two-tailed unpaired t-test, $p < 0.0001$. n = 6 mice for each group.

(N) ChR2-mediated stimulation of GABAergic PL neurons increased attack latency in RI. Two-tailed paired t-test, $p = 0.0107$. n = 9 mice for each group.

(O) ChR2-mediated stimulation of GABAergic PL neurons reduced attack bouts in RI. Two-tailed paired t-test, $p = 0.0004$, n = 9 mice for each group.

(P) ChR2-mediated stimulation of GABAergic PL neurons reduced attack duration in RI. Two-tailed paired t-test, $p = 0.0245$, n = 9 mice for each group.

(Q) ChR2-mediated stimulation of GABAergic PL neurons reduced pursuit bouts in RI. Two-tailed paired t-test, $p = 0.0081$, n = 9 mice for each group.

(R) ChR2-mediated stimulation of GABAergic PL neurons reduced pursuit duration in RI. Two-tailed paired t-test, $p = 0.0371$, n = 9 mice for each group. $^{*}p < 0.05$, $^{**}p < 0.01$, $^{***}p < 0.001$; All data were presented as means ± SEM.

AGGs was much higher than in NONs (Figure 1B). To better understand the role of specific PL cell types (glutamatergic versus GABAergic) in aggressive behavior. We conducted double immunohistochemistry and found that after RI exposure, the number of double-labelled glutamatergic neurons of the marker vesicular glutamate transporter 2 (VGlut2) c-Fos^{+} was higher, whereas the number of double-labelled GABAergic c-Fos^{+} neurons was lower in AGGs compared with NONs (Figures 1C and 1D). Similar with previous studies,[13,23] we found fewer GABAergic neurons (11.2%) than VGlut2 neurons (88.8%) in the PL (Figure 1E), and the proportion of GABAergic c-Fos^{+} neurons in the RI test was lower than that of VGlut2 c-Fos^{+} neurons (Figure 1F).

To confirm this phenomenon, we performed cell-type-specific fiber photometry to record their activity during the RI test. To do this, we injected AAV-mDlx-GCaMP6s into the PL of CD-1 mice and implanted a fiber above the infected cells. Three weeks after surgery (Figure 1G), AGGs displayed robust diminished GABAergic neuron activity at the initiation of an aggressive interaction (Figures 1I–1L), whereas GABAergic neuron activity remained invariable in the NONs group (Figures 1M–1P). The mDlx enhancer sequence is specifically expressed in all forebrain GABAergic interneurons and can be used in the context of recombinant adeno-associated virus to broadly and specifically target and manipulate GABAergic interneurons.[24] To determine the specificity of the mDlx enhancer, we injected AAV-mDlx-mCherry into the PL. Three weeks later, we found that a few cells expressing mCherry also expressed VGlut2 (~1.6%; Figures S2A and S2C). As expected, the majority of cells expressing mCherry also expressed GABA (~97.1%; Figures S2B and S2C).

To investigate whether PL GABAergic neurons are related to aggression *in vitro*, we injected AAV-mDlx-EGFP into the PL of CD-1 mice to label the GABAergic neurons in this region, and viruses were allowed 3 weeks for expression before whole-cell patch-clamp recordings (Figure 1H). The firing frequency of PL GABAergic neurons was significantly decreased in AGGs compared to NONs (Figures 1Q and 1R). In addition, we used a 50-pA depolarizing current injection in current-clamp mode based on responses to a 500 ms, and PL GABAergic neuron firing frequency was significantly reduced in AGGs compared to NONs (Figures 1S–1T).

Activation of prelimbic GABAergic neurons decreased aggression

Our next question was whether GABAergic PL neuronal activity is sufficient to elicit aggression and aggression CPP. We injected AAV-mDlx-hM3Dq-mCherry or AAV-mDlx-mCherry into the PL of AGGs and intraperitoneally injected them with clozapine-N-oxide (CNO) or vehicle to chemogenetically activate GABAergic neurons after 3 weeks of virus expression (Figures 2A and 2C). CNO treatment significantly increased GABAergic c-Fos^{+} expression in the PL after RI test (Figures 2D and 2E). Interestingly, aggressive behavior was significantly ameliorated by CNO treatment in AAV-mDlx-hM3Dq-mCherry infected AGGs (Figures 2F–2J). At the same time, chemogenetic activation of GABAergic neurons in the PL of AGGs (Figure S3A) promoted aversion to the intruder-paired context during aggression CPP (Figures S3B–S3E). As observed in NONs, chemogenetic activation of GABAergic PL neurons failed to promote aversion to the intruder-paired context during aggression CPP (Figures S3G–S3J).

To confirm this, we next used an optogenetic approach. We injected AAV-mDlx-hChR2-mCherry or AAV-mDlx-mCherry into the PL of AGGs (Figure 2K). Similar to the chemogenetic results, we found that blue light (473 nm, 25 Hz, 20-ms in width, 10–15 mW, Figure 2B) significantly increased GABAergic c-Fos^{+} expression in the PL after RI test (Figures 2L and 2M). Optogenetic activation of PL GABAergic neurons with ChR2 in AGGs significantly decreased aggressive behaviors in RI test (Figures 2N-2R).

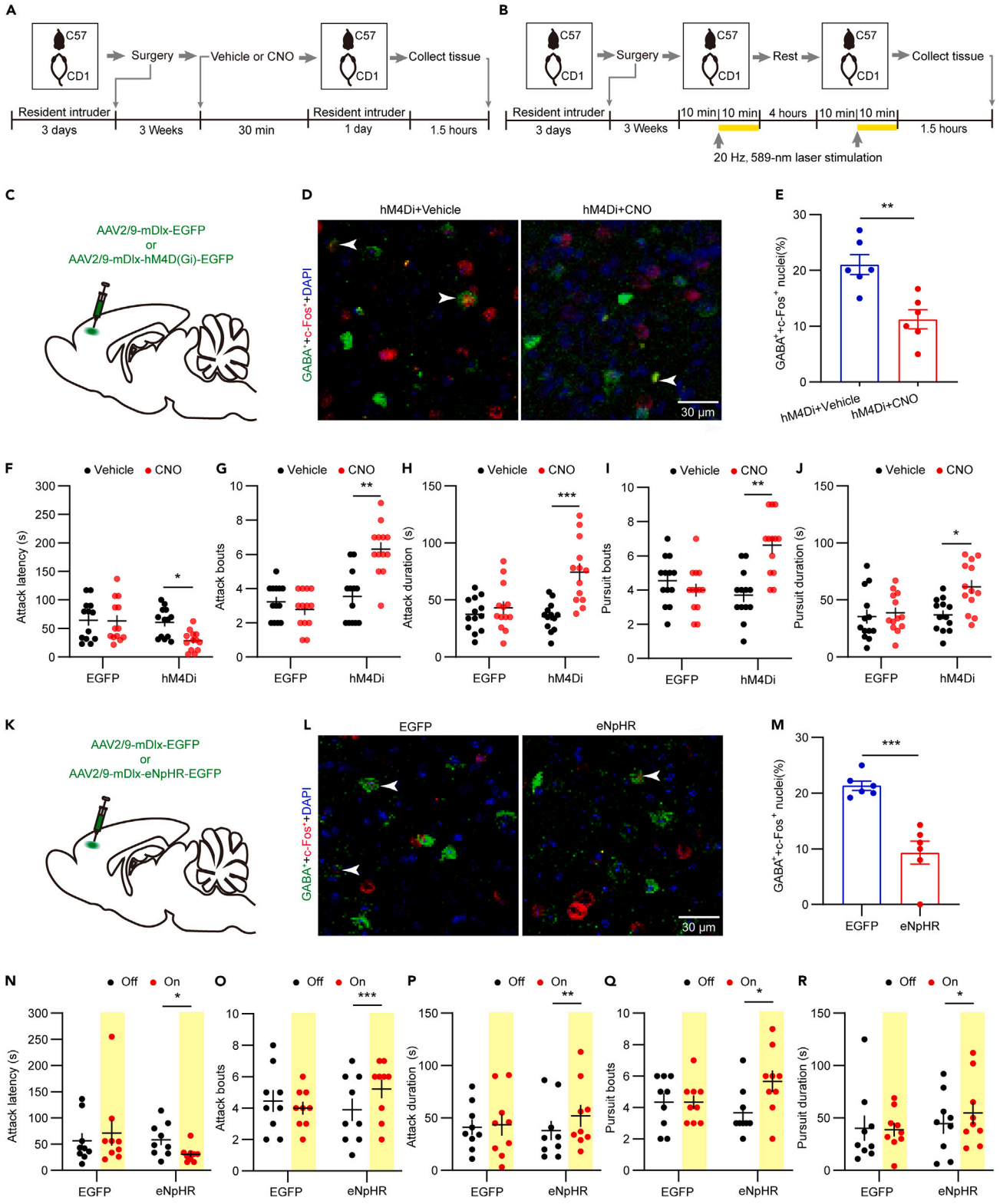

Figure 3. Opto and chemogenetics inhibition of PL GABAergic neurons increased aggressive behaviors

(A) Flowchart of an optogenetics inhibition experiment.

(B) Flowchart of an optogenetics inhibition experiment.

Figure 3. *Continued*

(C) Surgical manipulations and representative viral infection for GABAergic neuron in the PL.

(D) Representative images of immunofluorescence for EGFP (green), c-Fos (red) and DAPI (blue) in hM4Di+Vehicle group and hM4Di+CNO group (scale bar, 30 μm).

(E) CNO treatment reduced the percent of c-Fos$^+$ and GABA$^+$ co-expression neurons in hM4Di+CNO group compared to hM4Di +Vehicle group. Two-tailed unpaired t-test, p = 0.0026. n = 6 mice for each group.

(F) hM4Di-mediated stimulation of GABAergic PL neurons decreased attack latency after CNO treatment in RI. two-way ANOVA, p = 0.0460. n = 13 mice for each group.

(G) hM4Di-mediated stimulation of GABAergic PL neurons increased attack bouts after CNO treatment in RI. two-way ANOVA, p = 0.0024, n = 13 mice for each group.

(H) hM4Di-mediated stimulation of GABAergic PL neurons increased attack duration after CNO treatment in RI. two-way ANOVA, p = 0.0002, n = 13 mice for each group.

(I) hM4Di-mediated stimulation of GABAergic PL neurons increased pursuit bouts after CNO treatment in RI. two-way ANOVA, p = 0.0060, n = 13 mice for each group.

(J) hM4Di-mediated stimulation of GABAergic PL neurons increased pursuit duration after CNO treatment in RI. two-way ANOVA, p = 0.0107 n = 13 mice for each group.

(K) Surgical manipulations and representative viral infection for GABAergic neuron in the PL.

(L) Representative images of immunofluorescence for EGFP (green), c-Fos (red) and DAPI (blue) in EGFP group and eNpHR group (scale bar, 30 μm).

(M) Yellow light increased the percent of c-Fos$^+$ and GABA$^+$ co-expression neurons in eNpHR group compared to EGFP group. Two-tailed unpaired t-test, p = 0.0003. n = 6 mice for each group.

(N) eNpHR-mediated stimulation of GABAergic PL neurons reduced attack latency in RI. Two-tailed paired t-test, p = 0.0421. n = 9 mice for each group.

(O) eNpHR-mediated stimulation of GABAergic PL neurons increased attack bouts in RI. Two-tailed paired t-test, p = 0.0165, n = 9 mice for each group.

(P) eNpHR-mediated stimulation of GABAergic PL neurons increased attack duration in RI. Two-tailed paired t-test, p = 0.0039, n = 9 mice for each group.

(Q) eNpHR-mediated stimulation of GABAergic PL neurons increased pursuit bouts in RI. Two-tailed paired t-test, p = 0.0171, n = 9 mice for each group.

(R) eNpHR-mediated stimulation of GABAergic PL neurons increased pursuit duration in RI. Two-tailed paired t-test, p = 0.0446 n = 9 mice for each group.

*p < 0.05, **p < 0.01, ***p < 0.001; All data were presented as means ± SEM.

Inhibition of prelimbic GABAergic neurons elicited aggression

To determine whether PL GABAergic neurons contribute to aggression, we assayed if the chemogenetic inhibition of these neurons increases aggression and aggression CPP. We injected AAV-mDlx-hM4Di-EGFP or AAV-mDlx-EGFP into the PL of AGGs, and after 3 weeks of virus expression CNO treatment (Figures 3A and 3C) significantly reduced GABAergic c-Fos$^+$ expression in the PL after RI test (Figures 3D and 3E). Ethological analysis revealed that CNO-treated AGGs significantly increased aggressive behaviors (Figures 3F–3J). Chemogenetic inhibition of the PL of AGGs did not further elicit CPP for the intruder-paired context during aggression (Figures S3B and S3C) but did increase intruder-paired time (Figure S3F). As observed in NONs, chemogenetic inhibition of PL GABAergic neurons of NONs robustly promoted CPP in the intruder-paired context (Figures S3G, S3H, and S3K).

To confirm this, we next used an optogenetic approach to inhibit GABAergic neuronal activity in the PL. To do this, we injected AAV-mDlx-eNpHR-EGFP or AAV-mDlx-EGFP into the PL of AGGs (Figure 3K). As expected, we found that yellow light (589 nm, 20 Hz, 10-ms in width, 15–20 mW, Figure 3B) significantly decreased PL GABAergic c-Fos$^+$ expression after RI test (Figures 3L and 3M). Optogenetic inhibition of PL GABAergic neurons with eNpHR in AGGs increased aggressive behaviors (Figures 3N–3R).

Manipulation of GABAergic signaling in the lateral hypothalamus influences aggression

The PL sends projections to several of the brain areas linked to aggression, such as the hypothalamus, amygdala, periaqueductal gray (PAG) and dorsal raphe nucleus.[25–27] Next, we tested whether GABAergic PL neurons project to downstream areas and which of them are involved in aggression. We performed anterograde tracing of their projections by injecting AAV-mDlx-EGFP into the PL of CD-1 mice (Figure S4A), and we observed a prominent axonal projection of EGFP-positive axons in some regions, such as the internal capsule (IC) (Figure S4B), the nucleus of the horizontal limb of the diagonal band (HDB) (Figure S4C), and the LH area (Figure S4D). These results suggest that GABAergic PL neurons might directly target neurons in the major downstream regions of PL efferents.

To investigate whether PL GABAergic neurons projecting outside influence aggressive behavior, we injected AAV-mDlx-mCherry, AAV-mDlx-hChR2-mCherry, or AAV-mDlx-eNpHR-mCherry into the PL, and optogenetic stimulation of the axonal terminals of GABAergic PL neurons in the IC (Figure S5) or HDB (Figure S6) had no obvious effects on aggressive behavior. However, we found that blue light stimulation of GABAergic PL neuron axonal terminals in the LH of AGGs significantly reduced orexinergic c-Fos$^+$ expression (Figures 4A–4C) and inhibited mouse aggression (Figures 4D–4H). Whereas yellow light stimulation of GABAergic PL neuron axonal terminals in the LH of AGGs significantly increased orexinergic c-Fos$^+$ expression (Figures 4I–4K) and promoted mouse aggression (Figures 4L–4P).

Prelimbic GABAergic neurons project to lateral hypothalamus orexinergic meurons to regulate aggressive behavior

Then, we were curious about which type of neurons are the targets of long-term GABAergic projection from the PL. Considering that orexinergic neurons are strictly localized in the hypothalamus, particularly in the lateral hypothalamic area,[28] the orexinergic system plays an important role in the regulation of various motivated behaviors, from sleep arousal to social interaction.[21,29–31] Therefore, we proposed that GABA-mediated disinhibition of orexin signaling would promote aggressive behavior. We injected AAV-mDlx-mCherry or

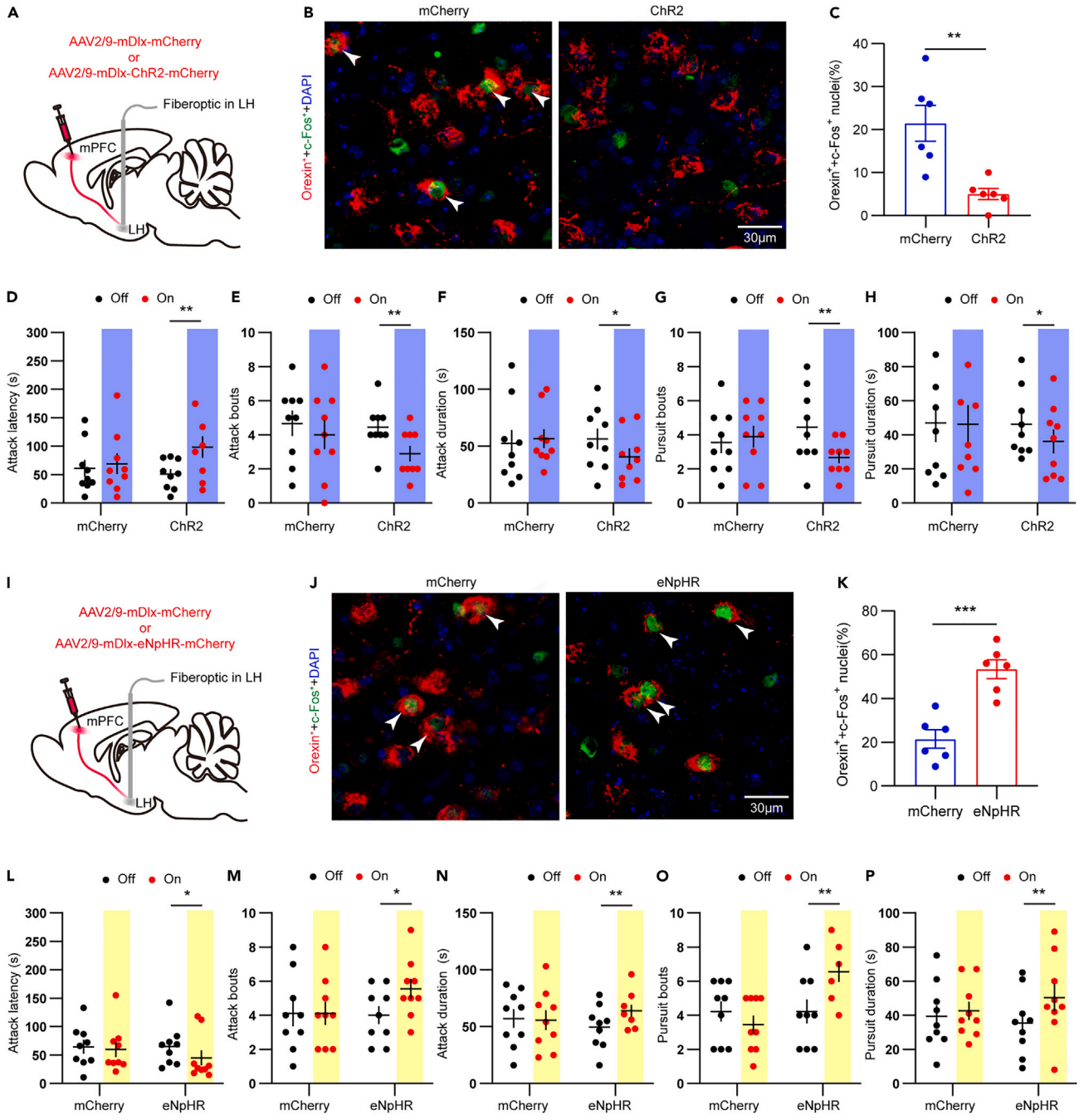

Figure 4. Optogenetic manipulation of GABAergic inputs to the LH modulates aggressive behavior in AGGs

(A) Schematic showing viral injection into the PL and optogenetic stimulation of GABAergic neuron terminals in the LH.

(B) Representative images of immunofluorescence for mCherry (orexinergic neuron, red), c-Fos (green), and DAPI (blue) in mCherry group and ChR2 group (scale bar, 30 μm).

(C) Blue light reduced the percent of c-Fos$^+$ and orexin$^+$ co-expression neurons in ChR2 group compared to mCherry group. Two-tailed unpaired t-test, p = 0.0037. n = 6 mice for each group.

(D) ChR2-mediated stimulation of GABAergic PL neurons increased attack latency in RI. Two-tailed paired t-test, p = 0.0046. n = 9 mice for each group.

(E) ChR2-mediated stimulation of GABAergic PL neurons reduced attack bouts in RI. Two-tailed paired t-test, p = 0.0081, n = 9 mice for each group.

(F) ChR2-mediated stimulation of GABAergic PL neurons reduced attack duration in RI. Two-tailed paired t-test, p = 0.0134, n = 9 mice for each group.

(G) ChR2-mediated stimulation of GABAergic PL neurons reduced pursuit bouts in RI. Two-tailed paired t-test, p = 0.0234, n = 9 mice for each group.

(H) ChR2-mediated stimulation of GABAergic PL neurons reduced pursuit duration in RI. Two-tailed paired t-test, p = 0.0010, n = 9 mice for each group.

(I) Schematic showing viral injection into the PL and optogenetic stimulation of GABAergic neuron terminals in the LH.

Figure 4. *Continued*

(J) Representative images of immunofluorescence for mCherry (orexinergic neuron, red), c-Fos (green), and DAPI (blue) in mCherry group and eNpHR group (scale bar, 30 μm).

(K) Yellow light increased the percent of c-Fos$^+$ and GABA$^+$ co-expression neurons in eNpHR group compared to mCherry group. Two-tailed unpaired t-test, $p = 0.0004$. n = 6 mice for each group.

(L) eNpHR-mediated stimulation of GABAergic PL neurons reduced attack latency in RI. Two-tailed paired t-test, $p = 0.0398$, n = 9 mice for each group.

(M) eNpHR-mediated stimulation of GABAergic PL neurons increased attack bouts in RI. Two-tailed paired t-test, $p = 0.0278$, n = 9 mice for each group.

(N) eNpHR-mediated stimulation of GABAergic PL neurons increased attack duration in RI. Two-tailed paired t-test, $p = 0.0057$, n = 9 mice for each group.

(O) eNpHR-mediated stimulation of GABAergic PL neurons increased pursuit bouts in RI. Two-tailed paired t-test, $p = 0.0037$, n = 9 mice for each group.

(P) eNpHR-mediated stimulation of GABAergic PL neurons increased pursuit duration in RI. Two-tailed paired t-test, $p = 0.0017$, n = 9 mice for each group.

*$p < 0.05$, **$p < 0.01$, ***$p < 0.001$; All data were presented as means ± SEM.

AAV-mDlx-hM3D(Gq)-mCherry into the PL to label GABAergic PL neurons (Figure 5A) in combination with orexin immunohistochemistry to visualize GABA-positive axons connected with orexinergic neurons in the LH (Figure 5B). Next, we recorded neurons at LH using whole-cell patch clamps in combination with intracellular biocytin labeling and immunohistochemistry to confirm that the recorded neurons were orexinergic neurons (Figures 5C and 5D).

We found that 5 μM CNO activation of GABAergic PL neurons with hM3D(Gq) in AGG mice significantly inhibited the firing rate of orexinergic neurons in the LH. Next, we used a 50 μM bicuculline bath to rescue the firing rate of orexinergic neurons in the LH. After a 2–3 min washout of bicuculline, the firing rate of orexinergic neurons in the LH was again reduced. Finally, we washed out CON from the perfusate, and the firing rate of orexinergic neurons in the LH recovered to the resting level (Figure 5F). However, the control virus could not induce these effects (Figure 5E). These results indicated that PL GABAergic neurons may reduce aggression through a long projection to LH orexigenic neurons.

Next, to determine whether orexinergic neurons in the LH are necessary for inter-male aggression, we used agonists or antagonists of the orexin receptor to record their activity during RI and aggression CPP (Figures 6A and 6B). To do this, we injected the agonist of both orexin-1 and orexin-2 receptors, orexin-A, into the lateral hypothalamus of AGGs, which triggered an increase in aggressive behavior (Figures 6C–6G). Orexin-A also elicited CPP for the intruder-paired context during aggression (Figures 6H–6J). On the contrary, intraperitoneal injection of the dual orexin receptor antagonist almorexant significantly decreased aggressive behavior (Figures 6K–6O) and showed conditioned place aversion in AGGs (Figures 6P–6R). These data support the conclusion that orexinergic neurons in LH are specifically involved in the regulation of aggressive behavior.

DISCUSSION

Acts of violence account for an estimated 1.43 million deaths worldwide annually,[32] but the mechanism behind aggression remains unclear. In this study, we performed a series of experiments to detect, and functionally prove the pivotal role of previously uncharacterized PL GABAergic neurons, and to characterize a downstream target - LH orexinergic neurons in modulating aggressive behavior. We identified an important role of GABAergic PL neurons as a "brake" in regulating aggression. Activating these neurons could inhibit aggressive behavior and reduce CPP in AGGs. Furthermore, we provided causal evidence for the anatomical and functional connectivity of the PL-LH circuit. The GABAergic PL-orexinergic LH projection is an important control circuit for intermale aggressive behavior, both of which may be targets for curbing aggression.

Initially, we used the RI test and CPP model to screen aggressive and non-aggressive CD-1 mice. The level of aggressive behavior often increases in the first trials but generally stabilizes after three trials. After repeated interactions with invader, AGGs exhibit increased serum testosterone and decreased corticosterone levels compared with NONs, suggesting that NONs may be less dominant. These results are similar to previous studies that found individual differences in aggressive behavior between antagonists in CD-1 mice.[2,21,33] Next, to search for aggression-activated nuclei, we detected c-Fos expression in the whole brain. c-Fos is an immediate-early gene that is generally used as a marker for activated neurons.[34] Our study found that bilateral PL nuclei were dramatically activated during aggression. This result agrees with previous studies showing that subdivisions of the prefrontal cortex become activated by fights in rodents and primates.[8,35–38] Although more glutamatergic neurons (88.8%) than GABAergic neurons (11.2%) were observed in the PL and the activity of the PL as a whole might be increased during aggression or in response to aggression-related cues, we identified a small subset of GABAergic c-Fos$^+$ PL neurons that were robustly inhibited in aggression behavior. These results add new insight into the complex, delicate regulatory role of PL in maintaining the balance of impulsive behavior.

Using *in vivo* fiber photometry to measure neuronal activity, we found that firing frequencies of GABAergic PL neurons were significantly decreased in AGGs compared with NONs. These results are consistent with the c-Fos results and a previous study showing that most activated cells in the PL of AGGs were glutamatergic cells, whereas the number of activated interneurons in the PL was decreased.[36] However, many questions about these neurons remain. First, do GABAergic PL neurons act as a brake in aggression? In the neocortex, 85–90% of neurons are pyramidal cells, and the rest are GABAergic inhibitory neurons.[23,39] GABAergic neurons are involved in regulation a wide range of neuroprocesses in the brain.[40] Here, we provide evidence that the direct optogenetic activation of GABAergic PL neurons of AGGs inhibits aggression and aggression CPP, whereas the optogenetic inhibition of GABAergic PL neurons of AGGs promotes aggression and aggression CPP. Similarly, using the chemogenetic activation of GABAergic PL neurons of AGGs promoted aversion of the intruder-paired context during aggression CPP, but this effect did not appear in NONs. Along with the finding that activated GABAergic neuron are increased in NONs

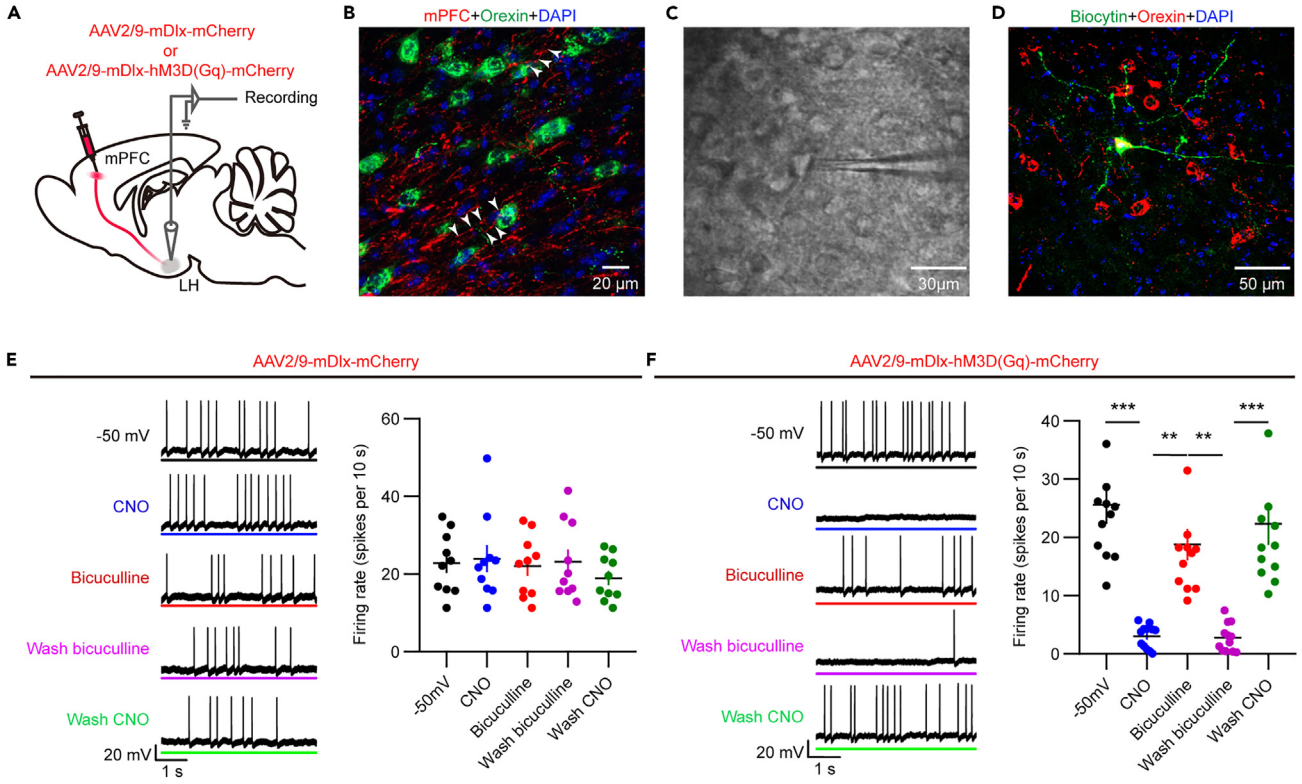

Figure 5. Validation of LH orexinergic neurons involved in regulating aggressive behavior

(A) Schematic showing viral injection into the PL and recording in the LH for (E)–(F).

(B) Representative images of immunofluorescence for orexin (green), terminals of GABAergic PL neuron (red) and DAPI (blue) after virus injection in PL (scale bar, 30 μm).

(C) Representative image of a typical LH neuron with the visible patch pipette (scale bar: 30 μm).

(D) Representative images of immunofluorescence for biocytin (green), orexin (red) and DAPI (blue) in LH (scale bar, 50 μm).

(E) Representative traces from an orexinergic neuron in the LH during baseline (top), CNO (Line 2), bicuculline (Line 3), wash bicuculline (Line 4), and wash CNO (bottom) conditions. Scatterplot representative the firing rate of orexinergic neurons in the LH firing. Kruskal-Wallis one-way ANOVA with repeated measures, n = 8 biologically independent mice, n = 12 cells, $p = 0.7826$.

(F) Representative traces from an orexinergic neuron in the LH during baseline (top), CNO (Line 2), bicuculline (Line 3), wash bicuculline (Line 4), and wash CNO (bottom) conditions. Scatterplot representative the firing rate of orexinergic neurons in the LH firing. Kruskal-Wallis one-way ANOVA with repeated measures, n = 8 biologically independent mice, n = 12 cells, $p < 0.0001$. Dunn's multiple-comparisons baseline versus orexin-A, adjusted $p < 0.0001$; CNO versus bicuculline, adjusted $p = 0.0041$; bicuculline versus wash bicuculline, adjusted $p = 0.0017$; wash bicuculline versus wash CNO, adjusted $p = 0.0002$.

during the aggression test as compared to AGGs, these results indicate that the further activation of PL GABAergic neurons did not alter the decision of non-aggression toward intruder in NONs. On the contrary, chemogenetic inhibition of GABAergic PL neurons of AGGs increased the duration of paired CPP. Chemogenic inhibition of hM4Di expressed GABAergic PL neurons in NONs also significantly increased the paired time in the CPP of NONs. These results provide evidence that the GABAergic neurons of the PL are involved in the modulation of aggression behavior. The few activated GABAergic PL neurons in AGGs did provide some control toward violent behavior. Inhibition of these neurons could escalate aggressive behavior, while the disinhibition of the PL GABAergic neurons in the "peace maker" NONs could also elicit aggression-like behavior. Therefore, we believe that GABAergic PL neurons act as a brake in aggressive behavior. When exposed to an intruder, AGGs exhibit decreased activity of GABAergic PL neurons as compared to NONs, contributing to a behavioral preference for environmental contexts associated with the interaction. This is the first study to provide functional evidence that GABAergic PL neurons produce inhibitory control to regulate aggressive interactions. Second, the question remains whether there is top-down projection-specific connectivity in aggression. Notably, two major outputs of the PL, the PAG projections and the nucleus accumbens (NAc), were previously implicated in social defeat and acute avoidance behavior, respectively.[41,42] Decreased top-down control by cortical areas is thought to underlie pathological forms of aggression.[43,44] In our study, anterograde tracing showed prominent axonal projection of GABAergic PL neurons to the IC, HDB, and LH. However, only the manipulation of the LH terminals of PL GABAergic projections affected aggression. Our results agree with a recent study suggesting that PL-LH neurons modulate dominance through social competition.[4]

The next question is which kind of neurons in LH participate in the aggressive behavior? The LH comprises a diversity of cell types and has been shown to drive hypersocial behavior and social investigation,[45] as well as modulate social defensive behaviors.[46,47] Interestingly, studies

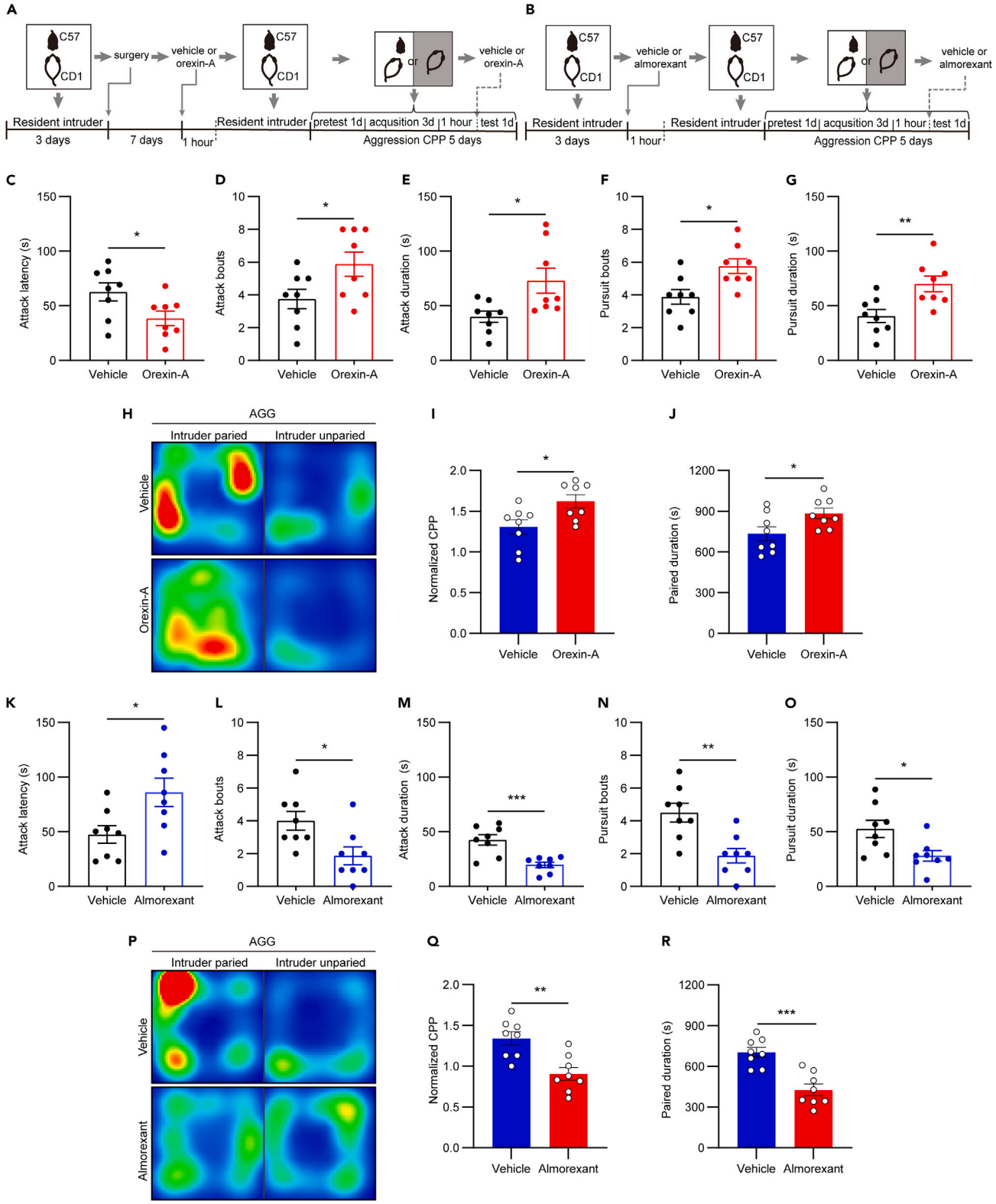

Figure 6. LH orexinergic neurons involved in regulating aggressive behavior

(A) Flowchart of the orexin-A activation experiment.

(B) Flowchart of the almorexant inhibition experiment.

Figure 6. *Continued*

(C) Activation of orexinergic LH neurons decreased attack latency after orexin-A treatment in RI. Two-tailed unpaired t-test, p = 0.0385, n = 8 mice for each group.
(D) Activation of orexinergic LH neurons increased attack bouts after orexin-A treatment in RI. Two-tailed unpaired t-test, p = 0.0418, n = 8 mice for each group.
(E) Activation of orexinergic LH neurons increased attack duration after orexin-A treatment in RI. Two-tailed unpaired t-test, p = 0.0194, n = 8 mice for each group.
(F) Activation of orexinergic LH neurons increased pursuit bouts after orexin-A treatment in RI. Two-tailed unpaired t-test, p = 0.0102, n = 8 mice for each group.
(G) Activation of orexinergic LH neurons increased pursuit duration after orexin-A treatment in RI. Two-tailed unpaired t-test, p = 0.0071, n = 8 mice for each group.
(H) Representative CPP heatmaps for Vehicle and orexin-A in AGGs.
(I) Normalized CPP score in AGGs. Two-tailed unpaired t-test, p = 0.0204, n = 8 mice for each group.
(J) Duration of the intruder paired. Two-tailed unpaired t-test, p = 0.0359, n = 8 mice for each group.
(K) Inhibition of orexinergic signaling increased attack latency after almorexant treatment in RI. Two-tailed unpaired t-test, p = 0.0241, n = 8 mice for each group.
(L) Inhibition of orexinergic signaling reduced attack bouts after almorexant treatment in RI. Two-tailed unpaired t-test, p = 0.0175, n = 8 mice for each group.
(M) Inhibition of orexinergic signaling reduced attack duration after almorexant treatment in RI. Two-tailed unpaired t-test, p = 0.0008, n = 8 mice for each group.
(N) Inhibition of orexinergic signaling reduced pursuit bouts after almorexant treatment in RI. Two-tailed unpaired t-test, p = 0.0026, n = 8 mice for each group.
(O) Inhibition of orexinergic signaling reduced pursuit duration after almorexant treatment in RI. Two-tailed unpaired t-test, p = 0.0186, n = 8 mice for each group.
(P) Representative CPP heatmaps for Vehicle and almorexant in AGGs.
(Q) Normalized CPP score in AGGs. Two-tailed unpaired t-test, p = 0.0018, n = 8 mice for each group.
(R) Duration of the intruder paired. Two-tailed unpaired t-test, p = 0.0002, n = 8 mice for each group. *p < 0.05, **p < 0.01, ***p < 0.001; All data were presented as means ± SEM.

have found that orexinergic neuron cell bodies are localized exclusively in the LH.[48,49] There is evidence that orexin signaling in the lateral habenula (LHb) GABAergic neurons regulate aggression reward,[21] which is similar to several other studies demonstrating a role of orexin in other motivated behaviors, such as win fights.[50] Inhibition of orexin signaling reduces CPP,[51] self-administration[52] and relapse for abusive drugs.[30,53,54] Thus, we hypothesized that GABAergic PL neurons may project onto orexinergic LH neurons to elicit aggressive control. As expected, GABAergic PL neurons directly project to LH orexinergic neurons. The *ex vivo* experiments suggested that the chemogenetic activation of GABAergic axon terminals coming from the PL with CNO significantly altered the orexinergic neuron firing rate in the LH. Bicuculline reversed the CNO-induced orexinergic neuron firing in the LH. This result suggests PL GABA transmission exert orexinergic modulation effects in the LH. Furthermore, when GABAergic axonal terminals from the PL were optogenetically inhibited in LH, aggressive behaviors were promoted, while the activation of this projection significantly reduced aggressive behaviors in mice. All these results confirmed that GABAergic PL neurons project to orexinergic LH neurons to regulate aggressive behavior. Furthermore, are LH orexinergic neurons directly involved in the aggressive behavior? To answer this question, we performed a pharmacological experiment to directly activate LH-orexinergic neurons by orexin-A. The results showed that the mice exhibited more aggressive behavior and had a CPP for the intruder-paired context. However, blocking the orexin receptor significantly reduced the aggressive behavior of mice and displayed conditioned place aversion. These data support the conclusion that orexinergic neurons in LH are specifically involved in the regulation of aggressive behavior.

Collectively, we show that GABAergic PL neurons play an important role in modulating aggression and preference for aggression-paired contexts through the disinhibition of orexinergic LH neurons. Our results provide new insights into the neural circuitry of territorial aggression behavior. Further elucidation of how neuronal populations in the brain affect the generation and modulation of aggressive behaviors is needed.

Limitations of study

Notably, GABAergic neurons in the PL are composed of several subsets of functionally distinguished interneurons including parvalbumin-expressing (PV), somatostatin-expressing (SST), cholecystokinin (CCK), and vasoactive intestinal polypeptide (VIP) positive neurons.[14,55–57] To better understand this PL-LH circuit in aggression, it is important to identify the specific subtype of interneurons that accounts for projection to the LH and modulation of aggression. To be noted, there is also limitation to this study that all the experiments in the current study were conducted during the light phase, which is a period of lower activity levels for nocturnal rodents. Previous studies suggest that orexin signal in the LH exhibits circadian control, which may influence the regulation of aggressive behavior in different phases.[31,58] Even though the mechanism has not been fully elucidated, aggressive behaviors do vary during light and dark conditions.[59] Future study exploring whether light-dark cycle influences the PL-LH circuit on aggressive behavior is warranted.

STAR★METHODS

Detailed methods are provided in the online version of this paper and include the following:

- KEY RESOURCES TABLE
- RESOURCE AVAILABILITY
  - Lead contact
  - Materials availability
  - Data and code availability
- EXPERIMENTAL MODEL AND STUDY PARTICIPANT DETAILS
  - Animals
  - Experimental design

SUPPLEMENTAL INFORMATION

Supplemental information can be found online at https://doi.org/10.1016/j.isci.2023.107718.

ACKNOWLEDGMENTS

This research was supported by grants from National Natural Science Foundation of China (82101273 to F.B. and 82171265 to H.L.), Postdoctoral Research Foundation of China (2021M693936 to F.B.), Project of Chongqing Natural Science Foundation Postdoctoral Science Foundation (cstc2021jcyj-bshX0071 to F.B.), and Army Medical University Youth Incubation Program (2021XQN19 and 20QNPY014 to F.B.).

AUTHOR CONTRIBUTIONS

H.L. and Y.X. conceptualized the project, designed, and supervised experiments, and wrote the article. F.B. performed most experiments, analyzed data, and wrote the initial draft of the article. L.H. performed some recording and tracing experiments. J.D. performed all immediate-early gene mapping experiments. Z.L., X.H., and P.C. performed tracing experiments. G.W. and H.W. provided expertise in the resident-intruder paradigm. Q.D. analyzed some data. X.B. and J.H. performed some ELISA and immunofluorescent staining. M.Y., D.L., Y.R., and M.Z. assisted with video annotation and image analysis.

DECLARATION OF INTERESTS

The authors declare no competing interests.

INCLUSION AND DIVERSITY

We support inclusive, diverse, and equitable conduct of research.

Received: January 12, 2023
Revised: June 6, 2023
Accepted: August 22, 2023
Published: August 25, 2023

REFERENCES

1. Zhang, Z., Zhang, Y., Yuwen, T., Huo, J., Zheng, E., Zhang, W., and Li, J. (2022). Hyperexcitability of corticothalamic PT neurons in mPFC promotes irritability in the mouse model of Alzheimer's disease. Cell Rep. *41*, 111577. https://doi.org/10.1016/j.celrep.2022.111577.
2. Golden, S.A., Heshmati, M., Flanigan, M., Christoffel, D.J., Guise, K., Pfau, M.L., Aleyasin, H., Menard, C., Zhang, H., Hodes, G.E., et al. (2016). Basal forebrain projections to the lateral habenula modulate aggression reward. Nature *534*, 688–692. https://doi.org/10.1038/nature18601.
3. Amodio, D.M., and Frith, C.D. (2006). Meeting of minds: the medial frontal cortex and social cognition. Nat. Rev. Neurosci. *7*, 268–277. https://doi.org/10.1038/nrn1884.
4. Padilla-Coreano, N., Batra, K., Patarino, M., Chen, Z., Rock, R.R., Zhang, R., Hausmann, S.B., Weddington, J.C., Patel, R., Zhang, Y.E., et al. (2022). Cortical ensembles orchestrate social competition through hypothalamic outputs. Nature *603*, 667–671. https://doi.org/10.1038/s41586-022-04507-5.
5. Zhou, T., Zhu, H., Fan, Z., Wang, F., Chen, Y., Liang, H., Yang, Z., Zhang, L., Lin, L., Zhan, Y., et al. (2017). History of winning remodels thalamo-PFC circuit to reinforce social dominance. Science *357*, 162–168. https://doi.org/10.1126/science.aak9726.
6. Wang, F., Zhu, J., Zhu, H., Zhang, Q., Lin, Z., and Hu, H. (2011). Bidirectional control of social hierarchy by synaptic efficacy in medial prefrontal cortex. Science *334*, 693–697. https://doi.org/10.1126/science.1209951.
7. Nelson, R.J., and Trainor, B.C. (2007). Neural mechanisms of aggression. Nat. Rev. Neurosci. *8*, 536–546. https://doi.org/10.1038/nrn2174.
8. Takahashi, A., Nagayasu, K., Nishitani, N., Kaneko, S., and Koide, T. (2014). Control of intermale aggression by medial prefrontal cortex activation in the mouse. PLoS One *9*, e94657. https://doi.org/10.1371/journal.pone.0094657.
9. Raine, A., Buchsbaum, M., and LaCasse, L. (1997). Brain abnormalities in murderers indicated by positron emission tomography.

Biol. Psychiatry *42*, 495–508. https://doi.org/10.1016/S0006-3223(96)00362-9.

10. Damasio, H., Grabowski, T., Frank, R., Galaburda, A.M., and Damasio, A.R. (1994). The return of Phineas Gage: clues about the brain from the skull of a famous patient. Science *264*, 1102–1105. https://doi.org/10.1126/science.8178168.
11. Anderson, S.W., Bechara, A., Damasio, H., Tranel, D., and Damasio, A.R. (1999). Impairment of social and moral behavior related to early damage in human prefrontal cortex. Nat. Neurosci. *2*, 1032–1037. https://doi.org/10.1038/14833.
12. Wei, J., Zhong, P., Qin, L., Tan, T., and Yan, Z. (2018). Chemicogenetic Restoration of the Prefrontal Cortex to Amygdala Pathway Ameliorates Stress-Induced Deficits. Cereb. Cortex *28*, 1980–1990. https://doi.org/10.1093/cercor/bhx104.
13. Rudy, B., Fishell, G., Lee, S., and Hjerling-Leffler, J. (2011). Three groups of interneurons account for nearly 100% of neocortical GABAergic neurons. Dev. Neurobiol. *71*, 45–61. https://doi.org/10.1002/dneu.20853.
14. Xu, X., Roby, K.D., and Callaway, E.M. (2010). Immunochemical characterization of inhibitory mouse cortical neurons: three chemically distinct classes of inhibitory cells. J. Comp. Neurol. *518*, 389–404. https://doi.org/10.1002/cne.22229.
15. Haider, B., and McCormick, D.A. (2009). Rapid neocortical dynamics: cellular and network mechanisms. Neuron *62*, 171–189. https://doi.org/10.1016/j.neuron.2009.04.008.
16. Klausberger, T., and Somogyi, P. (2008). Neuronal diversity and temporal dynamics: the unity of hippocampal circuit operations. Science *321*, 53–57. https://doi.org/10.1126/science.1149381.
17. Wehr, M., and Zador, A.M. (2003). Balanced inhibition underlies tuning and sharpens spike timing in auditory cortex. Nature *426*, 442–446. https://doi.org/10.1038/nature02116.
18. Pouille, F., and Scanziani, M. (2001). Enforcement of temporal fidelity in pyramidal cells by somatic feed-forward inhibition. Science *293*, 1159–1163. https://doi.org/10.1126/science.1060342.
19. McBain, C.J., and Fisahn, A. (2001). Interneurons unbound. Nat. Rev. Neurosci. *2*, 11–23. https://doi.org/10.1038/35049047.
20. Falkner, A.L., Grosenick, L., Davidson, T.J., Deisseroth, K., and Lin, D. (2016). Hypothalamic control of male aggression-seeking behavior. Nat. Neurosci. *19*, 596–604. https://doi.org/10.1038/nn.4264.
21. Flanigan, M.E., Aleyasin, H., Li, L., Burnett, C.J., Chan, K.L., LeClair, K.B., Lucas, E.K., Matikainen-Ankney, B., Durand-de Cuttoli, R., Takahashi, A., et al. (2020). Orexin signaling in GABAergic lateral habenula neurons modulates aggressive behavior in male mice. Nat. Neurosci. *23*, 638–650. https://doi.org/10.1038/s41593-020-0617-7.
22. Sallet, J., Mars, R.B., Noonan, M.P., Andersson, J.L., O'Reilly, J.X., Jbabdi, S., Croxson, P.L., Jenkinson, M., Miller, K.L., and Rushworth, M.F.S. (2011). Social network size affects neural circuits in macaques. Science *334*, 697–700. https://doi.org/10.1126/science.1210027.
23. Zhong, S., Zhang, S., Fan, X., Wu, Q., Yan, L., Dong, J., Zhang, H., Li, L., Sun, L., Pan, N., et al. (2018). A single-cell RNA-seq survey of the developmental landscape of the human prefrontal cortex. Nature *555*, 524–528. https://doi.org/10.1038/nature25980.
24. Dimidschstein, J., Chen, Q., Tremblay, R., Rogers, S.L., Saldi, G.A., Guo, L., Xu, Q., Liu, R., Lu, C., Chu, J., et al. (2016). A viral strategy for targeting and manipulating interneurons across vertebrate species. Nat. Neurosci. *19*, 1743–1749. https://doi.org/10.1038/nn.4430.
25. Hoover, W.B., and Vertes, R.P. (2011). Projections of the medial orbital and ventral orbital cortex in the rat. J. Comp. Neurol. *519*, 3766–3801. https://doi.org/10.1002/cne.22733.
26. Gabbott, P.L.A., Warner, T.A., Jays, P.R.L., Salway, P., and Busby, S.J. (2005). Prefrontal cortex in the rat: projections to subcortical autonomic, motor, and limbic centers. J. Comp. Neurol. *492*, 145–177. https://doi.org/10.1002/cne.20738.
27. Vertes, R.P. (2004). Differential projections of the infralimbic and prelimbic cortex in the rat. Synapse *51*, 32–58. https://doi.org/10.1002/syn.10279.
28. Huber, M.J., Chen, Q.H., and Shan, Z. (2018). The Orexin System and Hypertension. Cell. Mol. Neurobiol. *38*, 385–391. https://doi.org/10.1007/s10571-017-0487-z.
29. Lazaridis, I., Tzortzi, O., Weglage, M., Märtin, A., Xuan, Y., Parent, M., Johansson, Y., Fuzik, J., Fürth, D., Fenno, L.E., et al. (2019). A hypothalamus-habenula circuit controls aversion. Mol. Psychiatry *24*, 1351–1368. https://doi.org/10.1038/s41380-019-0369-5.
30. Tung, L.W., Lu, G.L., Lee, Y.H., Yu, L., Lee, H.J., Leishman, E., Bradshaw, H., Hwang, L.L., Hung, M.S., Mackie, K., et al. (2016). Orexins contribute to restraint stress-induced cocaine relapse by endocannabinoid-mediated disinhibition of dopaminergic neurons. Nat. Commun. *7*, 12199. https://doi.org/10.1038/ncomms12199.
31. Ren, S., Wang, Y., Yue, F., Cheng, X., Dang, R., Qiao, Q., Sun, X., Li, X., Jiang, Q., Yao, J., et al. (2018). The paraventricular thalamus is a critical thalamic area for wakefulness. Science *362*, 429–434. https://doi.org/10.1126/science.aat2512.
32. Siever, L.J. (2008). Neurobiology of aggression and violence. Am. J. Psychiatry *165*, 429–442. https://doi.org/10.1176/appi.ajp.2008.07111774.
33. Koolhaas, J.M., Coppens, C.M., de Boer, S.F., Buwalda, B., Meerlo, P., and Timmermans, P.J. (2013). The resident-intruder paradigm: a standardized test for aggression, violence and social stress. J. Vis. Exp. *77*, e4367. https://doi.org/10.3791/4367.
34. Jiang-Xie, L.F., Yin, L., Zhao, S., Prevosto, V., Han, B.X., Dzirasa, K., and Wang, F. (2019). A common neuroendocrine substrate for diverse general anesthetics and aleep. Neuron *102*, 1065. https://doi.org/10.1016/j.neuron.2019.03.033.
35. Takahashi, A., and Miczek, K.A. (2014). Neurogenetics of aggressive behavior: studies in rodents. Curr. Top. Behav. Neurosci. *17*, 3–44. https://doi.org/10.1007/7854_2013_263.
36. Halász, J., Tóth, M., Kalló, I., Liposits, Z., and Haller, J. (2006). The activation of prefrontal cortical neurons in aggression–a double labeling study. Behav. Brain Res. *175*, 166–175. https://doi.org/10.1016/j.bbr.2006.08.019.
37. Haller, J., Tóth, M., Halasz, J., and De Boer, S.F. (2006). Patterns of violent aggression-induced brain c-fos expression in male mice selected for aggressiveness. Physiol. Behav. *88*, 173–182. https://doi.org/10.1016/j.physbeh.2006.03.030.
38. Hosokawa, T., and Watanabe, M. (2012). Prefrontal neurons represent winning and losing during competitive video shooting games between monkeys. J. Neurosci. *32*, 7662–7671. https://doi.org/10.1523/JNEUROSCI.6479-11.2012.
39. Freund, T.F., and Buzsaki, G. (1996). Interneurons of the hippocampus. Hippocampus *6*, 347–470. https://doi.org/10.1002/(SICI)1098-1063(1996)6:4<347::AID-HIPO1>3.0.CO;2-I.
40. Pi, H.J., Hangya, B., Kvitsiani, D., Sanders, J.I., Huang, Z.J., and Kepecs, A. (2013). Cortical interneurons that specialize in disinhibitory control. Nature *503*, 521–524. https://doi.org/10.1038/nature12676.
41. Lee, A.T., Vogt, D., Rubenstein, J.L., and Sohal, V.S. (2014). A class of GABAergic neurons in the prefrontal cortex sends long-range projections to the nucleus accumbens and elicits acute avoidance behavior. J. Neurosci. *34*, 11519–11525. https://doi.org/10.1523/JNEUROSCI.1157-14.2014.
42. Franklin, T.B., Silva, B.A., Perova, Z., Marrone, L., Masferrer, M.E., Zhan, Y., Kaplan, A., Greetham, L., Verrechia, V., Halman, A., et al. (2017). Prefrontal cortical control of a brainstem social behavior circuit. Nat. Neurosci. *20*, 260–270. https://doi.org/10.1038/nn.4470.
43. Blair, R.J.R. (2013). The neurobiology of psychopathic traits in youths. Nat. Rev. Neurosci. *14*, 786–799. https://doi.org/10.1038/nrn3577.
44. Jager, A., Amiri, H., Bielczyk, N., van Heukelum, S., Heerschap, A., Aschrafi, A., Poelmans, G., Buitelaar, J.K., Kozicz, T., and Glennon, J.C. (2020). Cortical control of aggression: GABA signalling in the anterior cingulate cortex. Eur. Neuropsychopharmacol *30*, 5–16. https://doi.org/10.1016/j.euroneuro.2017.12.007.
45. Nieh, E.H., Vander Weele, C.M., Matthews, G.A., Presbrey, K.N., Wichmann, R., Leppla, C.A., Izadmehr, E.M., and Tye, K.M. (2016). Inhibitory Input from the Lateral Hypothalamus to the Ventral Tegmental Area Disinhibits Dopamine Neurons and Promotes Behavioral Activation. Neuron *90*, 1286–1298. https://doi.org/10.1016/j.neuron.2016.04.035.
46. Rangel, M.J., Jr., Baldo, M.V.C., Canteras, N.S., and Hahn, J.D. (2016). Evidence of a Role for the Lateral Hypothalamic Area Juxtadorsomedial Region (LHAjd) in Defensive Behaviors Associated with Social Defeat. Front. Syst. Neurosci. *10*, 92. https://doi.org/10.3389/fnsys.2016.00092.
47. Li, Y., Zeng, J., Zhang, J., Yue, C., Zhong, W., Liu, Z., Feng, Q., and Luo, M. (2018). Hypothalamic Circuits for Predation and Evasion. Neuron *97*, 911–924.e5. https://doi.org/10.1016/j.neuron.2018.01.005.
48. Gautvik, K.M., de Lecea, L., Gautvik, V.T., Danielson, P.E., Tranque, P., Dopazo, A., Bloom, F.E., and Sutcliffe, J.G. (1996). Overview of the most prevalent hypothalamus-specific mRNAs, as identified by directional tag PCR subtraction. Proc. Natl. Acad. Sci. USA *93*, 8733–8738. https://doi.org/10.1073/pnas.93.16.8733.
49. Peyron, C., Tighe, D.K., van den Pol, A.N., de Lecea, L., Heller, H.C., Sutcliffe, J.G., and Kilduff, T.S. (1998). Neurons containing hypocretin (orexin) project to multiple neuronal systems. J. Neurosci. *18*, 9996–10015.

50. Nakajo, H., Chou, M.Y., Kinoshita, M., Appelbaum, L., Shimazaki, H., Tsuboi, T., and Okamoto, H. (2020). Hunger Potentiates the Habenular Winner Pathway for Social Conflict by Orexin-Promoted Biased Alternative Splicing of the AMPA Receptor Gene. Cell Rep. *31*, 107790. https://doi.org/10.1016/j.celrep.2020.107790.

51. Sartor, G.C., and Aston-Jones, G.S. (2012). A septal-hypothalamic pathway drives orexin neurons, which is necessary for conditioned cocaine preference. J. Neurosci. *32*, 4623–4631. https://doi.org/10.1523/JNEUROSCI.4561-11.2012.

52. Shoblock, J.R., Welty, N., Aluisio, L., Fraser, I., Motley, S.T., Morton, K., Palmer, J., Bonaventure, P., Carruthers, N.I., Lovenberg, T.W., et al. (2011). Selective blockade of the orexin-2 receptor attenuates ethanol self-administration, place preference, and reinstatement. Psychopharmacology *215*, 191–203. https://doi.org/10.1007/s00213-010-2127-x.

53. Harris, G.C., Wimmer, M., and Aston-Jones, G. (2005). A role for lateral hypothalamic orexin neurons in reward seeking. Nature *437*, 556–559. https://doi.org/10.1038/nature04071.

54. Gentile, T.A., Simmons, S.J., Barker, D.J., Shaw, J.K., España, R.A., and Muschamp, J.W. (2018). Suvorexant, an orexin/hypocretin receptor antagonist, attenuates motivational and hedonic properties of cocaine. Addict. Biol. *23*, 247–255. https://doi.org/10.1111/adb.12507.

55. Pinto, L., and Dan, Y. (2015). Cell-Type-Specific Activity in Prefrontal Cortex during Goal-Directed Behavior. Neuron *87*, 437–450. https://doi.org/10.1016/j.neuron.2015.06.021.

56. Kvitsiani, D., Ranade, S., Hangya, B., Taniguchi, H., Huang, J.Z., and Kepecs, A. (2013). Distinct behavioural and network correlates of two interneuron types in prefrontal cortex. Nature *498*, 363–366. https://doi.org/10.1038/nature12176.

57. Tremblay, R., Lee, S., and Rudy, B. (2016). GABAergic Interneurons in the Neocortex: From Cellular Properties to Circuits. Neuron *91*, 260–292. https://doi.org/10.1016/j.neuron.2016.06.033.

58. Saper, C.B., Scammell, T.E., and Lu, J. (2005). Hypothalamic regulation of sleep and circadian rhythms. Nature *437*, 1257–1263. https://doi.org/10.1038/nature04284.

59. Todd, W.D., Fenselau, H., Wang, J.L., Zhang, R., Machado, N.L., Venner, A., Broadhurst, R.Y., Kaur, S., Lynagh, T., Olson, D.P., et al. (2018). A hypothalamic circuit for the circadian control of aggression. Nat. Neurosci. *21*, 717–724. https://doi.org/10.1038/s41593-018-0126-0.

60. Mang, G.M., Dürst, T., Bürki, H., Imobersteg, S., Abramowski, D., Schuepbach, E., Hoyer, D., Fendt, M., and Gee, C.E. (2012). The dual orexin receptor antagonist almorexant induces sleep and decreases orexin-induced locomotion by blocking orexin 2 receptors. Sleep *35*, 1625–1635. https://doi.org/10.5665/sleep.2232.

STAR★METHODS

KEY RESOURCES TABLE

REAGENT or RESOURCE	SOURCE	IDENTIFIER
Antibodies		
Rabbit polyclonal anti-*c*-fos	Abcam	Cat# ab190289; RRID: AB_2737414
Mouse monoclonal anti-Vglut2	Sigma-Aldrich	Cat# MAB5504; RRID: AB_2187552
Rabbit polyclonal anti-GABA	Sigma-Aldrich	Cat# A2052; RRID: AB_477652
Rat monoclonal anti-*c*-Fos	Synaptic Systems	Cat# 226017; RRID: AB_2864765
Rat polyclonal anti-Orexin	Sigma-Aldrich	Cat# AB3704; RRID: AB_91545
Chemicals, peptides, and recombinant proteins		
CNO	Sigma-Aldrich	C0832
Orexin-A	Abmole Bioscience	M9573
Almorexant	Abmole Bioscience	M3261
Critical commercial assays		
Testosterone ELISA Kit	Abnova	KA6128
Corticosterone ELISA Kit	Abnova	KA6129
Software and algorithms		
VisuTrack	Shanghai Xinruan	https://www.shxinruan.com/dwxwfxrj/2.html
Photometry signal algorithm	Thinkerbiotech	http://www.thinkerbiotech.com/

RESOURCE AVAILABILITY

Lead contact

Further information and requests for resources and reagents should be directed to and will be fulfilled by the lead contact, Hong Li (lh78553@163.com).

Materials availability

There are no new unique reagents or restrictions on availability.

Data and code availability

- Confocal data files reported in this paper will be shared by the lead contact upon request.
- This paper does not report original code.
- Any additional information required to reanalyze the data reported in this paper is available from the lead contact upon request.

EXPERIMENTAL MODEL AND STUDY PARTICIPANT DETAILS

Animals

Male CD-1 (ICR) mice (30–40 g) were 3 months old. The male and female should be housed together in a cage at least one week before testing. Subjects were confirmed to have equal access, experience and success as breeders. Male C57BL/6J mice were obtained at 8 weeks of age and used as novel intruders. All mice were obtained from Beijing Weitong Lihua Experimental Animal Technology Co., Ltd. CD-1 mice were single housed, and C57BL/6J mice were group housed. Mice were maintained on a 12 h light/dark cycle at 21 $\pm$ 2°C with *ad libitum* access to food and water. All animal procedures were approved by the Ethics Committee for Animal Experimentation of the Army Medical University and in accordance with the National Institutes of Health Guide for the Care and Use of Laboratory Animals.

Experimental design

Experiment 1. aggression screening

After a habituation period of seven days, male CD-1 mice were subjected to RI testing for three consecutive days, and then an aggression CPP was performed. The aggression CPP lasted five days (pretest 1 day, acquisition 3 days, and final test 1 day). On the 16th day, the open field test was performed. To assay testosterone or corticosterone after 24 h of the final screening (Figure S1A).

Experiment 2. effects of aggressive behavior on the activity of PL neurons

RI test for three consecutive days, 1.5 h after the end of the RI test on day 3, we detected the activity changes of glutamatergic and GABAergic neurons in PL by immunofluorescence in NONs and AGGs (Figure 1A). Then, we injected AAV2/9-mDlx-GCaMP6s and implanted optical fibers into the PL three weeks later to record GCaMP fluorescence signals in NONs and AGGs, respectively (Figure 1G). Finally, we injected AAV-mDlx-EGFP into the PL and performed whole-cell patch clamp recordings 3 weeks later. The firing frequency of GABAergic neurons in the PL was recorded in NONs and AGGs (Figure 1H).

Experiment 3. odulation of GABAergic PL neurons on aggressive behavior

Activation of GABAergic PL neurons: After RI testing for three consecutive days, we injected AAV2/9-mDlx-mCherry or AAV2/9-mDlx-hM3D(Gq)-mCherry into the PL. The experiment was divided into four groups: mCherry+vehicle, mCherry+CNO, hM3Dq+vehicle, hM3Dq+CNO. Three weeks later, we injected AGGs intraperitoneally either vehicle or CNO, and 30 min later RI test was performed. At 1.5 h after the end of the RI test, brain tissue was collected for immunofluorescence. In addition, we injected AAV2/9-mDlx-mCherry or AAV2/9-mDlx-hChR2-mCherry into the PL of AGGs. The experiment was divided into two groups: mCherry and ChR2. Three weeks later, we stimulated each AGG with blue light (473 nm) and compared the differences in RI assay between the two groups of mice before and after light administration. For the RI experiments, mice were tested twice on the same day (in a counterbalanced manner) under both light-on and light-off conditions, with at least 4 h between the two sessions. Brain tissue was collected 1.5 h after the end of the RI test for immunofluorescence (Figure 2A).

Inhibition of GABAergic PL neurons: After RI testing on three consecutive days, we injected AAV2/9-mDlx-EGFP or AAV2/9-mDlx-hM4D(Gi)-EGFP into the PL. The experiment was divided into four groups: EGFP+vehicle, EGFP+CNO, hM4Di+vehicle, hM4Di+CNO. Three weeks later, we injected AGGs intraperitoneally either vehicle or CNO, and 30 min later RI assay was performed. At 1.5 h after the end of the RI test, brain tissue was collected for immunofluorescence. In addition, we injected AAV2/9-mDlx-EGFP or AAV2/9-mDlx-eNpHR-EGFP into the PL of AGGs. The experiment was divided into two groups: EGFP and eNpHR. Three weeks later, we stimulated each AGG with yellow light (589 nm) and compared the differences in RI assay between the two groups of mice before and after light administration. For the RI experiments, mice were tested twice on the same day (in a counterbalanced manner) under both light-on and light-off conditions, with at least 4 h between the two sessions. Brain tissue was collected 1.5 h after the end of the RI test for immunofluorescence (Figure 2B).

For aggression CPP: After RI testing for three consecutive days, we injected AAV2/9-mDlx-mCherry, AAV2/9-mDlx-hM3D(Gq)-mCherry, or AAV2/9-mDlx-hM4D(Gi)-mCherry into the PL. The experiment was divided into three groups: mCherry, hM3Dq, hM4Di. Three weeks later, an aggression CPP was performed. After the pretest (1 day) and acquisition (3 days), the AGGs and NONs were injected intraperitoneally with CNO 30 min before the test on the test day (Figure S3A).

Experiment 4. manipulation of GABAergic PL-LH projection influences aggression

First, we injected AAV-mDlx-EGFP into the CD-1 mice to track the downstream areas of GABAergic PL neurons anterograde. Three weeks later, we sacrificed the mice and examined the whole brain for EGFG-positive axon expression. We then injected AAV-mDlx-mCherry, AAV-mDlx-hChR2-mCherry, or AAV-mDlx-eNpHR-mCherry into the PL. For the activation experiment, mice were divided into two groups depending on the virus: mCherry and ChR2. For the inhibition experiment, mice were divided into two groups depending on the virus: mCherry and eNpHR. Three weeks later, ChR2-or eNpHR-mediated simulation of axonal terminals of GABAergic PL neurons was performed in IC, HDB, and LH. The RI test was used to observe the changes in aggressive behavior of the mice.

To confirm that there was an anatomical connection and functional regulation in the PL-LH circuit, we injected AAV-mDlx-mCherry or AAV-mDlx-hM3D(Gq)- mCherry into the PL. Three weeks later, we examined the expression of GABA-positive axons with orexinergic neurons in LH. Next, we used the whole-cell patch-clamp technique to record orexigenic neurons in LH and observed the firing frequency of orexigenic neurons in LH under different conditions, i.e., −50mV→CNO→bicuculline→washout of bicuculline→washed out CON.

Experiment 5. manipulation of orexinergic LH neurons influences aggression

To activate orexinergic LH neurons, after RI testing on three consecutive days, AGGs were randomly assigned to a vehicle group and an orexin-A group. We implanted cannulae into the lateral hypothalamus, and seven days after surgery, we injected vehicle or orexin-A into the LH. Mice were then returned to home boxes, and the RI test was performed 1 h later. The aggression CPP was performed on the following five days, and orexin-A was administered 1 h before the test on the test day (Figure 6A).

To inhibit orexinergic LH neurons, after RI testing on three consecutive days, AGGs were randomly assigned to a vehicle group and an almorexant group. Almorexant was administered orally at a dose of 300 mg/kg on the experimental day, and the RI test was performed 1 h later. The aggression CPP was performed on the following five days, and almorexant was administered 1 h before the test on the test day (Figure 6B).

METHOD DETAILS

Aggression screening/RI test

House the resident male and the companion female together in the resident cage for at least one week prior to testing, CD-1 mice were exposed to a novel C57BL/6J intruder for 10 min daily over three consecutive days.[2] Each intruder presentation took place within the

home cage of the experimental mouse between 9:00 and 17:00 under white light conditions. During RI sessions, to allow unimpeded viewing and video recording of sessions, the cage top apparatus was removed. In CD-1 mice, it was determined that there would not be induction of stress-related or anxiety-related behaviors by choosing the duration and number of screening sessions. Video recorded (1) the latency to initial aggression, (2) the number of aggressive bouts, (3) the total duration of aggression, (4) the number of pursuit bouts, and (5) the total duration of pursuits. These behaviors are defined as follows[2,21]: initiation of aggression is defined by the first clear physical opponent interaction initiated by the CD-1 mouse, not including grooming or pursuit behavior. Aggressive duration is defined by an aggression cycle with continuous orientation of the CD-1 mouse toward the intruder. As soon as the resident mouse turned away from the intruder after initiating the attack, the attack was deemed completed. This definition allows for slight breaks (less than 5 s). AGGs were defined as CD-1 mice that initiated aggression during screening, and NONs were defined as mice that did not initiate any aggression during screening. Aggression screening was stopped if an intruder showed signs of injury. Ethological analysis of aggression behavior was performed by two blinded observers.

Aggression conditioned place preference (CPP)

After CD-1 mice screened with the RI test, an aggression CPP was performed on the fourth day. The aggression CPP task involved three phases: pretest, acquisition, and test. Before all testing, the mice were acclimated to the testing facility for 1 h. During all phases, red light was used, and sound abated. The CPP apparatus (Shanghai Xinruan) consisted of two unique conditioning chambers. One chamber had a white condition, and the other chamber had a black condition that allowed mice to enter either chamber unbiasedly. The software can automatically analyze the time of the movement track in the black box and in the white box and create two separate heat maps. In the pretest phase, mice were placed in one of the chambers of the conditioning apparatus and allowed to freely explore the apparatus for 20 min. In both chambers, there were no group differences in bias. For the acquisition phase, two conditioning trials were conducted daily for three continuous days, resulting in six acquisition trials. Experimental mice were confined to one chamber for 10 min in the presence or absence of a novel C57BL/6J intruder mouse during the morning (between 8:00 and 12:00) and afternoon (between 14:00 and 18:00) trials. The chamber conditions were counterbalanced among all groups. During the test day, mice were placed in either chamber without the presence of intruders and allowed to freely explore the apparatus for 20 min. To assess the behavior of aggression CPP data, we assessed (1) normalized CPP (duration of the test phase spent in the chamber with the intruder divided by the duration of the pretest phase spent in the intruder-paired chamber, taking into account behavior during both sessions) and (2) intruder-paired duration (duration of the test phase spent in the chamber with the intruder, accounting only the behavior during the test session).

Open field test

During the open field test, experimental mice were acclimated to the testing facility for 1 h before testing. Open field tests were performed in black Medical ABS Engineering Plastics (50 × 50 × 40 cm; Shanghai Xinruan) under red light conditions. Testing sessions lasted for 10 min. VisuTrack (Shanghai Xinruan) was used to record behavior such as the total distance traveled, time spent in the entire arena and time spent in the delineated center zones and corner zones.

Blood sampling and testosterone/corticosterone enzyme-linked immunosorbent assay (ELISA)

A submandibular vein bleed from mice was collected 24 h after the final screening. Serum testosterone (Abnova, Testosterone ELISA Kit) and corticosterone (Abnova, Corticosterone ELISA Kit) levels were assessed according to manufacturer specifications. After blood was collected in a serum separator tube and allowed to clot for 30 min at room temperature, it was centrifuged at 1,000 × g for 10 min and then stored frozen (−20°C) until analysis. The minimal detectable limit is 0.066 ng/mL for testosterone and 6.1 ng/mL for corticosterone.

Immunofluorescent staining and confocal microscopy

Mice were deeply anesthetized with 50 mg/kg pentobarbital sodium and transcardially perfused with 50 mL cold phosphate-buffered saline (PBS, pH 7.4) followed by fixation with 100 mL cold 4% paraformaldehyde (PFA) in PBS. The brains were carefully removed from the skull, fixed in 4% PFA for 12 h, and dehydrated with 20% and 30% sucrose overnight at 4°C. Continuous coronal sections were prepared on a freezing microtome (Leica) at 40 μm.

Slices were collected and stored in PBS at 4°C until immunofluorescent staining. Sections undergoing immunofluorescent staining were washed in PBS 3 times (5 min each time), and the brain slices were placed into 0.1% Triton X-100 to break the membrane for 1 h and then incubated in a blocking solution containing 5% normal goat serum in PBS for 1 h at room temperature. Slices were then incubated with primary antibodies in blocking solution at 4°C for 24 h. For primary antibodies, anti-rabbit c-fos (1:1000, ab190289, Abcam), anti-mouse VGlut2 (1:200, MAB5504, Sigma-Aldrich), anti-rabbit GABA (1:2000, A2052, Sigma-Aldrich), anti-rat c-Fos (1:1000, 226017, SYSY) and anti-rabbit Orexin (1:1000, AB3704, Sigma-Aldrich) were used. After primary antibody incubation, sections were washed with PBS 3 times (10 min each time) and incubated for 2 h in secondary antibody at room temperature. DyLight 488 goat anti-mouse IgG (1:500, Abbkine), DyLight 594 goat anti-rabbit IgG (1:500, Abbkine), DyLight 594 goat anti-rat IgG (1:500, Abbkine) and DyLight 488 goat anti-rabbit IgG (1:500, Abbkine) were used. After staining with DAPI for 10 min and washing 3 times (10 min each time) with PBS, sections were mounted on glass microscope slides, dried and covered with enhanced antifade mounting medium. Confocal images were acquired with an LSM 780 confocal microscope (Carl Zeiss, Jena, Germany) and further processed by Zen3.3 software (Zeiss).

In vitro electrophysiology

Mice used for *in vitro* electrophysiological recordings were anesthetized with pentobarbital sodium and decapitated, and the brain was removed immediately and submerged into ice-cold artificial cerebrospinal fluid (ACSF) containing (in mM) 124 NaCl, 3 KCl, 26 $NaHCO_3$, 2 $MgCl_2$, 2 $CaCl_2$, and 10 glucoses, adjusted to pH 7.2–7.4 and saturated with 95% O_2 and 5% CO_2. Coronal sections (300 μm thick) containing the PL or LH were sliced using a vibratome and allowed to equilibrate in recording ACSF oxygenated with 95% O_2 and 5% CO_2 for 1 h at room temperature. Then, sections were transferred to a recording chamber, where they were maintained at 31°C and perfused with oxygenated ACSF.

A whole-cell patch clamp experiment was performed on PL neurons expressing enhanced green fluorescent protein (EGFP), and the recording results were visualized with an upright microscope (Olympus, Japan) equipped with differential contrast optics, a 40× water immersion objective, and an infrared video imaging camera. In patch clamp recordings, capillary glass pipettes filled with an intrapipette solution containing (in mM) 125 potassium gluconate, 20 KCl, 10 HEPES, 1 EGTA, 2 $MgCl_2 \cdot 6H_2O$, and 4 ATP, adjusted to pH 7.2–7.4 with 1 KOH.

Whole-cell patch clamp recordings were obtained using a MultiClamp 700B amplifier (Axon Instruments, USA). Neurons that recorded rapidly activated and deactivated sodium currents in current-clamp mode were considered to have good performance. In current-clamp mode, recording the firing frequency of PL or LH neurons. A current waveform (−150 to 200 pA, 50 pA step, 500 ms) was injected into the recording GABAergic PL neuron. Signals were digitalized at 10 kHz and filtered at 2 kHz with Digidata 1440A/D (Axon Instruments, USA). Data were acquired and analyzed using Clampfit 10.7 software (Molecular Devices).

For characterization of the PL-to-LH connection, *in vitro* chemogenetically activating PL hM3D-mCherry neurons and the projected neurons in the LH were recorded. Action potentials were evoked in current-clamp configuration with the membrane potential holding to −50 mV. After recording baseline conditions for 2–3 min, 5 μM CNO (C0832, Sigma−Aldrich, USA) was continuously bath-applied, and 2 min later, 50 μM bicuculline methbromide (Sigma−Aldrich) was added for 2 min followed by washout. Bicuculline washout for 2–3 min followed by CNO washout. Offline analysis was performed using Clampfit 10.7 (Molecular Devices). Spikes were counted during baseline, CNO and bicuculline wash-in/out periods. To account for bath circulation, spikes were counted 2 min after the drug was added or after wash-out began.

Stereotaxic surgery and viral gene transfer

Mice (8–12 weeks old) were anesthetized with pentobarbital sodium (50 mg/kg, intraperitoneal injection, i.p.) and placed securely in a stereotaxic frame (RWD Life Technology Co. Ltd., China). To prevent drying and hard light, ophthalmic ointment was applied to the eyes. The scalp was shaved, cleaned with iodine and alcohol, and then incised to expose the skull. Drilling of small craniotomy holes (∼1 mm diameter) was performed under a microscope for virus injection. Nanoject II (Drummond Scientific, Broomall, PA) was used to inject virus through a micropipette opening of ∼20 μm. In the following procedure, 1 nL (1 nL/s) injections were made at 2 s intervals, resulting in a total of 100 nL. After injection, the virus was allowed to diffuse for 10 min before the needle was withdrawn. For PL injections, the coordinates from bregma were +2.1 mm AP, ±0.3 mm ML and −1.8 mm DV at a 0° angle.

For fiber photometry experiments, CD1 mice were injected unilaterally in the PL with AAV2/9-mDlx-GCaMP6s (Shanghai Taitool Bioscience Co., Ltd., China). The PL was implanted with optical fibers (FOC-W-2.5-200-0.37-2.0 mm, Inper) at the same time as the viral injection and secured with dental cement. For electrophysiology experiments, AAV2/9-mDlx-mCherry (a control virus that expressed only a fluorescent protein) or AAV2/9-mDlx-hM3D(Gq)-mCherry (that expressed a CNO sensitive, excitatory G protein–coupled receptor plus a fluorescent protein) was injected bilaterally into the PL (Shanghai Taitool Bioscience Co., Ltd., China). For optogenetic experiments, AAV2/9-mDlx-EGFP, AAV2/9-mDlx-mCherry, AAV2/9-mDlx-hChR2-mCherry (that expressed a blue light sensitive, excitatory G protein–coupled receptor plus a fluorescent protein), AAV2/9-mDlx-eNpHR-mCherry (that expressed a yellow light sensitive, inhibitory G protein–coupled receptor plus a fluorescent protein) or AAV2/9-mDlx-eNpHR-EGFP (Shanghai Taitool Bioscience Co., Ltd., China) was injected into the bilateral PL of CD1 mice, and the optic fibers (FOC-W-1.25-200-0.37-2.0/5.0 mm, Inper) were placed in the bilateral PL (+2.1 mm AP, ±0.3 mm ML and −1.65 mm DV), bilateral LH (−1.2 mm AP, ±1 mm ML and −4.7 mm DV), bilateral HDB (+0.5 mm AP, ±0.82 mm ML, −4.85 mm DV) or bilateral ic (−0.63 mm AP, ±1.63 mm ML, −3.6 mm DV). For chemogenetic experiments, AAV2/9-mDlx-EGFP, AAV2/9-mDlx-mCherry, AAV2/9-mDlx-hM3D(Gq)-mCherry, AAV2/9-mDlx-hM4D(Gi)-mCherry (that expressed a CNO sensitive, inhibitory G protein–coupled receptor plus a fluorescent protein) or AAV2/9-mDlx-hM4D(Gi)-EGFP (Shanghai Taitool Bioscience Co., Ltd., China) was injected into the bilateral PL of CD1 mice. Viruses were allowed at least 3 weeks for expression before electrophysiological or behavioral experiments. If viral transduction extended beyond the PL region, the data were excluded from analysis.

Fiber photometry

The optical fibers (NA = 0.37, Inper) were implanted into the PL (coordinates, bregma: AP = +2.1 mm; ML = +0.3 mm; DV = −1.7 mm, with a 0° angle toward the midline) at the same time as the viral injection and secured with dental cement. For at least two weeks, each mouse was housed separately to recover from the surgery and express the virus.

GCaMP fluorescence signals were recorded 3 weeks after surgery. Fluorescence emission was recorded with a fiber photometry system (Thinkerbiotech, Nanjing, China). To record GCaMP fluorescence signals, a 480 nm LED was used. A second 405-nm LED reflected autofluorescence and motion artifacts but did not correspond to GCaMP6s as a control. The laser power was adjusted to a low level of 15–25 μW at the tip of the fiber to minimize bleaching. The timeline for aggression photometry experiments was as follows: viral injection and optical fiber implantation (day 0), habituation to patch cord (days 15–21), and RI recordings (days 22–24). The mice were connected to the apparatus

and allowed to rest for 10 min before recording started. The GCaMP signal was allowed to stabilize for 2 min before the behavioral trial began. Each recording session lasted for 10 min.

Analysis: The photometry signal F was converted to $\Delta F/F = (V_{signal} - F_0)/(F_0 - V_{offset})$ baseline, where the baseline level was determined during the current recording period of the test. The resulting signals were analyzed by custom written MATLAB R2017b code (Thinkerbiotech, Nanjing, China), while the area under the curve per second of ΔF/F was calculated by GraphPad Prism 8 software.

Optogenetic stimulation

Before the optogenetic experiment, the mouse is connected to the optical cable and habituated to the optical cable for 1 h every day for at least 7 days. For blue light stimulation (ChR2), optical fibers were connected to a 473-nm blue laser diode (Intelligent optogenetic system, Newdoon) using a patch cord with an FC/PC adapter (250 mm O. D, NA = 0.37,2-m long, Thinkerbiotech, Nanjing, China). The intensity of the laser delivered to the brain was 10–15 mW. The PL, LH, HDB, and IC are optogenetically stimulated using pulses of 473-nm light, 20 ms in width, and 25 Hz, 15 s on and 15 s off.

For yellow light stimulation (NpHR), optical fibers were connected to a 589-nm yellow laser diode (Intelligent optogenetic system, Newdoon) to inhibit the neuron. A waveform generator was used to generate constant light pulses for 8 s followed by 2 s of light off. The intensity of the light delivered to the brain was 15–20 mW. The PL, LH, HDB, and IC are optogenetically inhibited using pulses of 589-nm light, 10 ms in width, and 20 Hz. For RI experiments, mice were tested twice on the same day (in a counterbalanced manner) in both light-on and light-off conditions, with at least 4 h between the two sessions.

Chemicals and drug administration

CNO (3 mg/kg, C0832, Sigma-Aldrich, USA) was dissolved in vehicle (1% dimethyl sulfoxide in saline) and injected intraperitoneally (i.p.) into the mice 30 min before the test. The control groups were injected with either vehicle or CNO. The crossover design ensured that the experimenters were blinded as to the drugs administered.

Implantation of cannulas in lateral hypothalamus

Mice were anesthetized with 50 mg/kg pentobarbital sodium and placed in a stereotaxic frame. The skull was exposed, and stainless-steel guide cannulae (diameter: 0.35 mm; length: 6 mm) were implanted bilaterally in the lateral hypothalamus using the following coordinates: +2.1 mm AP, ±0.3 mm ML, and −1.8 mm DV. The guide cannulae were fixed to the skull with dental cement and three anchoring screws. To prevent postoperative pain, the analgesic buprenorphine (0.01 mg/kg, intraperitoneally) was administered twice daily for the first two days after surgery. Behavioral testing began after complete recovery (7 days after surgery).

Drugs and injection

Orexin-A was purchased from Abmole Bioscience (AbMole, USA) and dissolved in sterile phosphate-buffered saline. A total volume of 0.3 μL solution containing 3 μg orexin-A was then injected at a flow rate of 0.1 μL/min, controlled by a Nanoject microinfusion pump II (Drummond Scientific, Broomall, PA).[60] After injection, the drugs were allowed to diffuse for 10 min before the needle was withdrawn. The mice were then returned to home boxes, and the RI test was performed 1 h later. The aggression CPP was performed on the following five days, and orexin-A was administered 1 h before the test on the test day.

Almorexant was purchased from Abmole Bioscience (AbMole, USA), dissolved in sterile water containing 0.25% methylcellulose, and administered orally at a dose of 300 mg/kg on the day of the experiment, and the RI test was performed 1 h later. The aggression CPP was performed on the following five days, and almorexant was administered 1 h before the test on the test day.

QUANTIFICATION AND STATISTICAL ANALYSIS

Data are presented as the mean ± SEM. Sample sizes were determined in accordance with previous publications on aggressive regulation in chemogenetics and optogenetics.[2,21] All statistical details can be found in the figure legends, including the type of statistical analysis used, p values, n, what n represents. Each dataset was tested for normality using the Shapiro–Wilk test. If the dataset passes the normality test, parametric tests are used. Otherwise, nonparametric tests are used.

For comparisons between two groups, paired or unpaired two-tailed Student's *t* tests were used. Mann–Whitney rank sum or Wilcoxon signed rank tests were used when the data were not normally distributed. For comparisons of three groups or more, one-way ANOVA was used, followed by a Bonferroni post hoc test. For nonparametric datasets, comparisons of three or more groups were performed using Kruskal–Wallis one-way ANOVA followed by Dunn's test for multiple comparisons. two-way ANOVA was used to analyze the effects of the two intervention factors and their interaction effects. We excluded data points if they were statistically significant outliers based on Grubb's test for outliers. Statistical analyses were performed using GraphPad Prism 8 software. Significant differences were set at $p < 0.05$.